Solar energy harvesting by magnetic-semiconductor nanoheterostructure in water treatment technology

Vahid Mahmoodi, Tahereh Rohani Bastami & Ali Ahmadpour

Environmental Science and Pollution Research

ISSN 0944-1344
Volume 25
Number 9

Environ Sci Pollut Res (2018)
25:8268-8285
DOI 10.1007/s11356-018-1224-y

Springer

Environmental Science and Pollution Research (2018) 25:8268–8285
https://doi.org/10.1007/s11356-018-1224-y

REVIEW ARTICLE

Solar energy harvesting by magnetic-semiconductor nanoheterostructure in water treatment technology

Vahid Mahmoodi[1] · Tahereh Rohani Bastami[2] · Ali Ahmadpour[1]

Received: 31 May 2017 / Accepted: 4 January 2018 / Published online: 25 January 2018

Abstract

Photocatalytic degradation of toxic organic pollutants in the wastewater using dispersed semiconductor nanophotocatalysts has a number of advantages such as high activity, cost effectiveness, and utilization of free solar energy. However, it is difficult to recover and recycle nanophotocatalysts since the fine dispersed nanoparticles are easily suspended in waters. Furthermore, a large amount of photocatalysts will lead to color contamination. Thus, it is necessary to prepare photocatalysts with easy separation for the reusable application. To take advantage of high photocatalysis activity and reusability, magnetic photocatalysts with separation function were utilized. In this review, the photocatalytic principle, structure, and application of the magnetic-semiconductor nanoheterostructure photocatalysts under solar light are evaluated.

Keywords Magnetic · Semiconductor · Nanoheterostrucutre · Core-shell · Heterojunction · Photocatalysis · Solar light

Introduction

The rate of clean water consumption has been much faster than the rate of population growth in the last century (Chong et al. 2010; Malato et al. 2009). Nowadays, clean water scarcity is one of the main challenges in many developing countries around the world. The rapid development of industrialization, population growth, and long-term droughts are some of factors that have deteriorated the situation caused by the lack of clean water (Chong et al. 2010). In both industrialized and developed countries, industrial effluents are one of the main pollutants released into the surface and underground waters, which contribute to the infiltration of contaminations such as heavy metals, pathogens, and organic compounds, among other things, in water supplies.

Therefore, the environment continues to be polluted at an increasing rate, and the traditional techniques of dealing with environmental pollution have been unable to meet the requirements of modern energy-saving issues and environmental protection (Wu et al. 2015). In this context, the development of wastewater treatment plants seems to offer a solution to the worldwide crisis. However, a closer analysis to this solution discloses more fundamental issues. For example, many wastewater treatment plants employ conventional purification methods such as chemical treatment (chlorination), adsorption, ultrafiltration, and biological treatments (active sludge), while the shortcomings and related problems of most of these methods have been shown (Lu et al. 2005; Magara et al. 1994, Marcucci et al. 2001; Nakada et al. 2006). It is necessary to find some attractive, low-cost, and highly efficient technologies to treat wastewater and eliminate contaminants in various effluents as much as possible.

In the last decade, advanced oxidation processes (AOPs) have been used for degradation of a wide range of water contaminants such as organic pollutants (dyes, pesticides, pharmaceuticals, herbicides, and so on) (Bastami and Ahmadpour 2016; Li et al. 2013; Rui et al. 2010; Toepfer et al. 2006), biorecalcitrant compounds (Hidalgo et al. 2011; Mahmoodi and Sargolzaei 2014b),

Highlights
- The magnetic-semiconductor nanoheterostructures and their recent applications on the water treatment technology are focused.
- The principle of the magnetic-semiconductor nanoheterostructure photocatalysts under solar light is described.
- The potential of magnetic-semiconductor nanomaterials is discussed.
- Magnetic core-shell and heterojunction structures are presented.

Responsible editor: Suresh Pillai

✉ Ali Ahmadpour
ahmadpour@um.ac.ir

[1] Department of Chemical Engineering, Faculty of Engineering, Ferdowsi University of Mashhad, Mashhad, Iran

[2] Department of Chemical Engineering, Faculty of Engineering, Quchan University of Technology, P.O. Box 94771-67335, Quchan, Iran

and pathogens (Chen et al. 2008; Singh et al. 2013). AOPs rely on the production of strong reactive oxidation species such as $^{\bullet}OH$ and $^{\bullet}O_2^-$, which can convert even the persistent molecules into biodegradable components (Oppenländer 2003). In fact, in the AOP processes, tough contaminants and toxic compounds are reduced to the extent that the purified wastewater could be released into surface streams or at least refined with conventional treatment methods.

In most cases, reactive radicals are produced in some consecutive reactions by means of a light source (e.g., UV or visible light) (Rosenfeldt and Linden 2004), some oxidants (e.g., H_2O_2, O_3, or O_2) (Trapido et al. 1997; Yeber et al. 1999), and/or photocatalysts (e.g., semiconductors such as TiO_2 and ZnO) (Mahmoodi and Sargolzaei 2014a). Since there are various ways of performing $^{\bullet}OH$ radical production, AOPs include different systems such as UV, UV/H_2O_2, UV/O_3, UV/H_2O_2/O_3, UV/photocatalyst, UV/H_2O_2/photocatalyst, and visible light/photocatalyst (Chong et al. 2010; Deng and Zhao 2015; Stasinakis 2008).

As a different type of AOP, heterogeneous visible light photocatalysis has attracted growing attention due to the versatility of the process, low cost, economic flexibility, environmental favorability, and high capability in wastewater treatment (Ibhadon and Fitzpatrick 2013). In other words, when traditional methods are not able to remove some special compounds (like organic molecules) in industrial effluents (either in terms of type or level of contamination), there should be another technology capable of reducing the concentration of these contaminants to the standard level. For instance, many researches have coupled the Fenton process with biological oxidation, which enhances degradation efficiency for organic Fenton combined with biological nitrification. Also, denitrification system has been evaluated in the treatment of a sanitary landfill leachate containing persistent organic matter such as humic and fulvic acids, xenobiotics, pesticides, and other harmful pollutants. The results suggest that the biological denitrification and nitrification system are unable to completely eliminate the organic compounds. However, after the photo-Fenton pre-treatment, the biological oxidation treatment showed great potentials to remove recalcitrant compounds.

In recent years, increasing attention has been paid to the application of semiconductor materials as photocatalysts for degradation of low concentrations of organic and inorganic molecules from aqueous or gas phase systems in fresh water treatment, environmental remediation, industrial, and health applications. However, it also suffers from shortcomings such as the separation of photocatalyst from the purified solution for reuse (Akhundi and Habibi-Yangjeh 2015; Liu et al. 2016). Magnetic heterogeneous photocatalysts offer a solution to this problem since a component with magnetic properties (such as Fe_2O_3, Fe_3O_4, and $CoFe_2O_4$) is incorporated in the structure of hybrid photocatalyst (Akhundi and Habibi-Yangjeh 2015; Hamad et al. 2015; Hankare et al. 2011; Liu et al. 2016; Sathishkumar et al. 2013; Yu et al. 2015). The magnetic component plays various roles in the performance of photocatalyst. The hybrid photocatalysts can simply be separated by an external magnetic field. In addition, the magnetic component may act as charge collector and inhibit the recombination of photo-excited electrons and holes. In other words, the exceptional properties of magnetic visible light photocatalysts provide a promising approach for environmental pollution control.

In this review, first the structure and mechanism of photocatalysis and solar light-induced degradation are described. Then, the potentials of magnetic-semiconductor nanomaterials are discussed. Finally, the nanoheterostructure of magnetic-semiconductor and their recent application in the water treatment technology are addressed.

Mechanism and structure of magnetic photocatalytic nanoheterostructure

Photocatalysis mechanism

Photocatalysis refers to the photoreactions rate (oxidation/reduction) brought on by the activation of a catalyst, usually a semiconductor oxide, via illumination under ultraviolet (UV) or visible light (Wu et al. 2015). The use of semiconductor oxide nanomaterial-based photocatalysts to degrade organic pollutants has been one of the most promising areas of research (Chen and Mao 2007; Liu et al. 2011). Photocatalysts are used in solid-liquid reaction systems, especially for the treatment of toxic waste. Heterogeneous photocatalysis is a promising method for the degradation of organic pollutants in water. The term "photocatalytic activity" came into use before the 1980s, when photocatalysis studies had attracted increasing attention thanks to the so-called Honda-Fujishima effect on the photoelectrochemical water splitting using a titanium oxide semiconductor electrode (Hoffmann et al. 1995).

As the photocatalysis reaction mechanism, the photoabsorption of a semiconductor excites electrons from the valence band (VB) to the conduction band (CB), which creates a positive hole in the VB, namely electron-hole pair (e^--h^+) generation (Fig. 1).

This interband (band-to-band) excitation is often described by three bands: VB, forbidden band (band gap), and CB. Also, there is site trapping of e^- or h^+ in the crystal lattice, so that e^- and h^+ are trapped by these sites "immediately" after the band-to-band transition, i.e., photoabsorption. The location of e^- and h^+ in the initial stage of photocatalysis as well as the rate

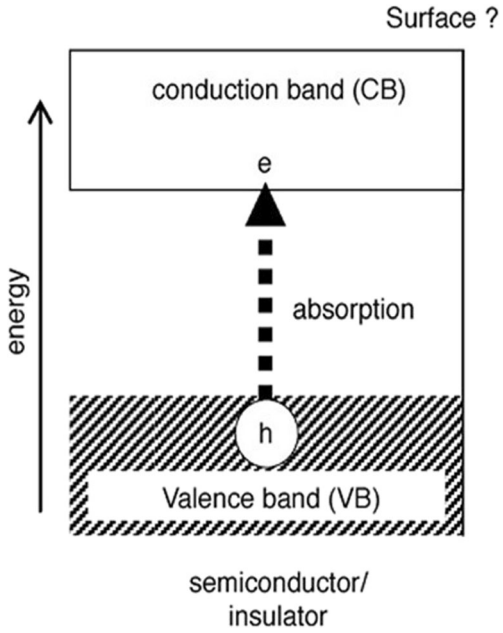

Fig. 1 Photoabsorption by transition of electrons in the valence band (VB) to the conduction band (CB) in a semiconductor (Augugliaro et al. 2006)

should be controlled by the spatial distribution of these traps in the photocatalysis (Augugliaro et al. 2006).

Fermi level is a measure of electrochemical potential of electron in a solid material (Rajeshwar et al. 2008). The Fermi level is below the CB and above the VB for n-type and p-type semiconductors, respectively (Augugliaro et al. 2006). In 1980s, it was found that this inner electric field led to the separation of e^--h^+ (Fig. 1).

In the case of photocatalytic processes in aqueous solutions, water and hydroxide ions react with photogenerated h^+ to form hydroxyl radicals ($^{\bullet}OH$), which are the primary oxidant in the photocatalytic oxidation of organic compounds (Chatterjee and Dasgupta 2005; Fujishima et al. 2007). $^{\bullet}OH$ ($E_0 = 2.80$ V vs. NHE) has higher oxidation potentials than other oxidants such as ozone (O_3) ($E_0 = 2.07$ V) and hydrogen peroxide (H_2O_2) ($E_0 = 1.77$ V) (Chatterjee and Dasgupta 2005). The $^{\bullet}OH$ can be generated in two processes: first, the O_2 present in water is reduced to form $^{\bullet}O_2^-$, which then reacts with H^+ to produce $^{\bullet}OOH$, followed by rapid degradation to $^{\bullet}OH$. The second process is the oxidation of OH^-.

It should be noted that redox reactions are induced by photo-excited electrons (e^-) and positive holes (h^+). Given the recombination of e^- and h^+ with each other, the overall photocatalytic reaction rate depends on the recombination rate. It is suggested that k_{redox} and $k_{recombination}$ are the rate constants of reactions by e^- and h^+ and their recombination, respectively. The ratio of $k_{redox}/k_{recombination}$ should be a measure of photocatalytic activity (Augugliaro et al. 2006). The recombination of a photo-excited electron (e^-) and a positive hole (h^+) is to some degree possible in photocatalysts, which can reduce quantum efficiency (Rajeshwar et al. 2008).

Optical band gap can be estimated using the following equation:

$$\alpha \propto \frac{(h\nu - E_g)^n}{h\nu} \quad or \quad (\alpha\nu)^{1/n} \propto h\nu - E_g \tag{1}$$

where α, h, ν, E_g, and n are the absorption coefficient, Planck constant, oscillation frequency, optical band gap, and constant of transition mode, respectively. The constant n is 1/2, 3/2, or 2 for allowed direct transition, forbidden direct transition, and forbidden indirect transition, respectively (Chatterjee and Dasgupta 2005).

However, there are certain limitations to large-scale applications of semiconductor oxide photocatalysts including (1) high recombination rate of electron-hole pairs, which leads to low quantum yield of the semiconductor photocatalysts (Liu and Li 2014) and (2) the limited harvesting of visible and solar light. Generally, wide-band gap semiconductor oxides are used as photocatalysts, i.e., the band gap value of anatase TiO_2 is 3.2 eV, which limits the light absorption of the UV region.

Combination of solar light-based process with other activation systems

It is clear that depending on the type of pollutant, using one process to purify different wastewaters will lead to operational failure. One way to solve this problem is to design a combined process for multistage removal of persistent pollutants. Recently, to increase the efficiency of visible light photocatalytic agents, many combined processes have been suggested including solar light/H_2O_2 process (Ndounla and Pulgarin 2015), solar photo-Fenton and solar-Fenton combined method (Aljubourya et al. 2016), and solar/electro-Fenton process (Liŭ et al. 2016). Topac and Alkan investigated the function of two solar-based processes, solar/H_2O_2 and solar photo-Fenton systems, in the inactivation of *Escherichia coli* bacteria in domestic wastewater (Topac and Alkan 2016).

In both methods, the H_2O_2 concentration and radiation intensity were key parameters affecting the process. It was found that both processes were highly efficient for *E. coli* disinfection, offering a good candidate for the inactivation of many bacterial species. Also, solar photo-Fenton system, solar photocatalyst, and solar photocatalyst of TiO_2/Fenton processes were used to treat petroleum wastewater along with a comparison of their performance. The value of total organic carbon (TOC) and chemical oxygen demand (COD) was measured and the effect of some operational parameters such as pH, Fenton agent type, and TiO_2 concentration was evaluated

by a central composite design (CCD). The results suggested that for solar photocatalysis of TiO_2 and TiO_2/Fenton system, TiO_2 concentration and pH were the two main parameters increasing the TOC and COD removal, while in the case of solar photo-Fenton process, pH and H_2O_2 dosages are the major parameters (Aljubourya et al. 2016).

Recently, Gutierrez-Mata et al. compared solar photocatalysis and solar photo-Fenton processes in terms of principles, performance, advantages, drawbacks, and applications. They discussed the activation process of every process precisely (Gutierrez-Mata et al. 2017).

Solar and visible light-induced photocatalysis

Since some nanophotocatalyst like titania can absorb only UV light, many researchers have developed this absorption range to the visible light region to utilize sunlight radiation as a free source of energy for photocatalysis (Dong et al. 2014; Liu et al. 2012b).

In solar radiation, the wavelength of light is in the range of 280 to 4000 nm. Thus, using photocatalysts which absorb light in the visible and near infrared regions is preferred. In addition, longer wavelengths of light carry lower energy, leading to a decrease in the potential for redox reactions (Jiang et al. 2016; Zapata-Torres et al. 2015).

Basically, the solar spectrum covers only 5–7% UV light, while 46 and 47% of the spectrum consist of visible light and infrared radiation, respectively (see Fig. 2) (Casbeer et al. 2012).

Visible light constitutes a large fraction of solar energy, so one of the great challenges in photocatalyst field is the design of new catalysts that exhibit high activity under illumination by visible/solar light. For the system to focus on the photocatalytic application under solar light and effectively absorb visible solar light energy, a maximum band gap of 3.1 eV is required (Xu et al. 2012).

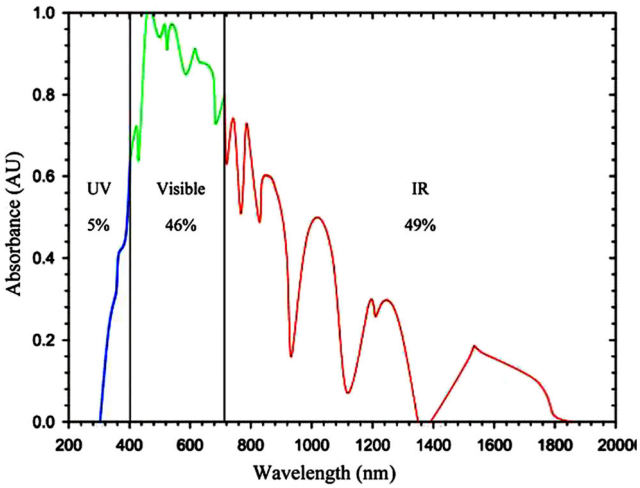

Fig. 2 Solar energy spectrum (Casbeer et al. 2012)

There are two pathways for the application of visible light irradiation by photocatalysts (Tang et al. 2004). One is doping UV active photocatalyst with elements in an attempt to make them active under visible light irradiation (Martyanov et al. 2004; Yang et al. 2005). "Doping" has been a keyword in the preparation of visible light-sensitive photocatalysts. In the case of photocatalysts with poor visible light activity, some modifications can be conducted with metal or non-metal elements to make them active under visible light irradiation. Doping refers to the insertion of atoms or ions in a crystalline lattice, i.e., modification of the bulk structure of crystallites rather than surface modification (Augugliaro et al. 2006).

The second approach is designing materials with a narrow band gap, which allows for photocatalytic activity under visible/solar light irradiation (Sun et al. 2008; Zhu et al. 2007). It is preferred to use narrow-band gap semiconductors rather than those with a wide band gap to utilize solar visible energy. Photocatalysts such as TiO_2 (Xu et al. 2007), ZnS (Kitano and Hara 2010), and $SrTiO_3$ (Boumaza et al. 2010) are effective under UV irradiation due to their wide band gaps, while $CaFe_2O_4$ (Ida et al. 2010), $MgFe_2O_4$ (Dom et al. 2011), $ZnFe_2O_4$ (Boumaza et al. 2010), CdS, and WO_3 (Xu et al. 2007) are effective under visible light irradiation owing to their narrow band gap.

Magnetic nanophotocatalysis

The photocatalytic treatment of highly concentrated organic pollutants from industrial wastewater usually poisons the photocatalyst and results in deactivation. In addition, it is difficult to separate a pure semiconductor photocatalyst from the wastewater system (Lu et al. 2007), as it can further deactivates the photocatalysts. Therefore, developing a low-cost, highly efficient, and reusable photocatalysts has gained considerable attention (Laurent et al. 2008).

In addition, it facilitates the combination of magnetic nanomaterials with semiconductor nanomaterials to form a magnetic-semiconductor photocatalyst. In magnetic-semiconductor system, magnetic nanomaterials are responsible for separating the photocatalyst from the solution by an external magnetic field. Therefore, designing a magnetic-semiconductor photocatalytic system has a crucial role in both basic and applied researches. When a system focuses on magnetic recovery properties, the saturation magnetization value of magnetic nanoparticle should not be less than 1 emu g^{-1} to be separated by an external magnetic field for further reuse and recovery (Qu and Duan 2013).

When a system focuses on the photocatalytic performance, the magnetic nanoparticles should have a relatively narrow-band gap value. For example, goethite and hematite are often used as photocatalysis for their low band gap (2.2 eV). Furthermore, spinel ferrites, with the general formula of MFe_2O_4, where M indicates a metal cation, are chemically

stable and used in a variety of applications due to their magnetic properties (Guin et al. 2005; Li et al. 2009). Ferrites demonstrate photocatalytic properties for many industrial processes (Guin et al. 2005), such as oxidative dehydrogenation of hydrocarbons (Gibson and Hightower 1976), decomposition of alcohols, and hydrogen peroxide (Manova et al. 2004). Various metals can change the redox properties of the ferrites in their lattice structure. Some ferrites have a band gap that is capable of the absorption of visible light (Dom et al. 2011).

In general, an optimal magnetic-semiconductor photocatalytic system should have the following requirements: (1) The preparation process should be simple and facile with high yield. (2) The composite system should exhibit an enhanced photocatalytic performance. (3) The magnetic photocatalyst composites should be recycled by an external magnetic field, which provides convenient regeneration. (4) The composite should retain suitable photocorrosion resistance and be stable at room temperature at least for months (Wu et al. 2015).

Among magnetic nanoparticles, magnetic iron oxides have attracted growing research interest due to their wide range of applications (Laurent et al. 2008; Xu et al. 2012). Iron oxides are composed of Fe and O (Wu et al. 2015). Among iron oxides, hematite (α-Fe_2O_3), magnetite (Fe_3O_4), and maghemite (γ-Fe_2O_3) have many applications.

In general, magnetic nanoparticles with a single magnetic domain are transformed into superparamagnetic at the room temperature by reducing their size to the range of 2 to 20 nm, meaning that the thermal energy can overcome the anisotropy energy behavior of single nanoparticles (Ratner et al. 2006; Yoon and Krishnan 2011). The semiconductor coating on the surface of magnetic nanoparticles reduces magnetic saturation (M_s) (An et al. 2012; Naseroleslami et al. 2016).

Many preparation approaches have been utilized to synthesize magnetic MNPs, including co-precipitation (Mascolo et al. 2013; Massart 1981; Suh et al. 2012), high-temperature thermal decomposition (Amara et al. 2012; Park et al. 2005), hydrothermal and solvothermal method (Tian et al. 2011; Wu et al. 2010), sol-gel reactions, polyol method (Dong and Zhu 2002; Qi et al. 2011), microemulsion synthesis (Han et al. 2011; Ladj et al. 2013), sonochemical reaction (Bastami and Entezari 2013), microwave-assisted synthesis (Ai et al. 2010; Wu et al. 2011), and biosynthesis (Scheffel et al. 2006).

Magnetic-semiconductor heterostructure nanophotocatalyst

In comparison with single-component nanomaterials, multiple-component nanomaterials have attracted greater attention due to the synergistic effects between components, which can enhance the final catalytic performance. Currently, wide-band gap semiconductors with good photocatalytic performance are used to synthesize magnetic featured nanoheterostructures. In a magnetic-semiconductor composite system, the magnetic nanoparticle not only separates and recovers the photocatalyst but also creates narrow/wide-band gap semiconductor heterostructures, which can improve the separation of electron and hole pairs, thereby increasing the visible light photocatalytic efficiency. If magnetic nanoparticles are considered as the core, the structure of magnetic-semiconductor nanocomposite heterostructure can be simply divided into the following structures: core-shell, matrix-dispersed, Janus, and shell-core-shell structures (Fig. 3) (Wu et al. 2015).

In the core-shell structure, the magnetic nanoparticle, as a core, is encapsulated by a semiconductor layer which stabilizes the magnetic nanoparticle. Generally, the magnetic nanoparticles are not placed at the center of semiconductor, so that often a yolk structure is obtained (Liu et al. 2013; Scheffel et al. 2006). In the matrix-dispersed structure, several magnetic nanoparticles are coated by or dispersed in a semiconductor matrix (Wang et al. 2009b). In the Janus structure, one side is a magnetic nanoparticle and the other side is a semiconductor material. An anisotropic surface chemical can have many applications even without self-assembly (Mou et al. 2012; Zeng et al. 2013). The magnetic nanoparticles are placed between two functional semiconductor materials in the shell-core-shell structure. In this structure, the two-shell layers are composed of the same or different semiconductors or one layer is a non-semiconductor material (Wang et al. 2009a).

Magnetic nanoparticles should be embedded in non-magnetic layers to avoid aggregation of magnetic nanoparticles and make particular surface properties for specific applications. A study on the relationship between photocatalytic performance and the structure of nanocomposites is essential for numerous applications. Therefore, further studies are required for the design and controllable synthesis of the nanostructured photocatalysts as well as optimization of the microstructure and photocatalytic performance (Wu et al. 2013).

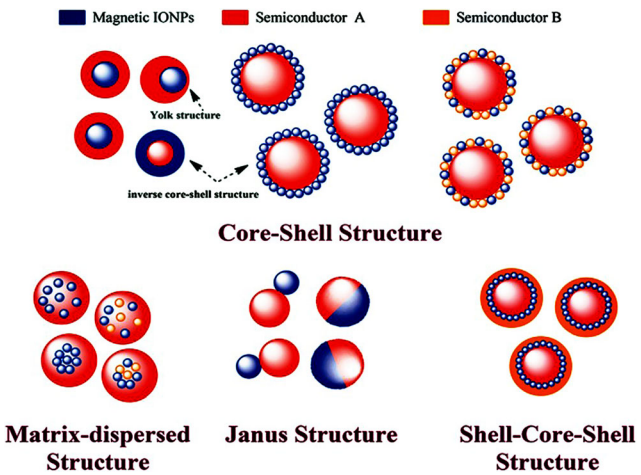

Fig. 3 Typical structure types of magnetic iron oxide-semiconductor composite nanomaterials. Blue spheres represent magnetic iron oxide nanoparticles, and the non-magnetic entities and matrix materials are displayed in other colors (Wu et al. 2015)

Recently, several magnetic-semiconductor photocatalytic nanostructures have been proposed, which can generally be sorted as core-shell and heterojunction structures. Actually, the magnetic components have crucial functions such as avoiding agglomeration of the catalyst nanoparticles during recovery and improving the catalytic activity (Xi et al. 2011). Various magnetic visible light photocatalysts have been used in degradation of organic molecules and their high degradation efficiency has been confirmed, as shown in Table 1.

In magnetic core-shell nanostructures, different magnetic sources such as Fe_3O_4 (Shekofteh-Gohari and Habibi-Yangjeh 2015; Yao et al. 2014a; Zhongliang et al. 2012), Fe_2O_3 (Huang et al. 2015a; Jang et al. 2014; Liu et al. 2012a), $CoFe_2O_4$ (Hamad et al. 2015), and $MgFe_2O_4$ (Tang et al. 2014) have been used. However, Fe_3O_4 is widely used due to its low-cost and desirable magnetic and non-toxic properties (Shekofteh-Gohari and Habibi-Yangjeh 2015).

On the other hand, one of the most efficient strategies for the improvement of visible light photocatalytic activity is semiconductor coupling and fabrication of different heterojunction structures such as Ag_2O-ZnO-Fe_3O_4 (Cai et al. 2015), Fe_3O_4@TiO_2/CdS (Wang et al. 2014), $\gamma Fe_2O_3/TiO_2$ (Mou et al. 2012), and $\alpha Fe_2O_3/TiO_2$ (Tang et al. 2013).

Synthetic approaches

A variety of methods have been used to synthesize various magnetic photocatalytic nanostructures. In this review, we discuss the synthetic approaches to magnetic-nanophotocatalyst-based core-shell structure and -based heterojunction structure. For core-shell magnetic nanocomposites, the core structure is a magnetic component, which in most cases, is synthesized by a simple precipitation method (Yao et al. 2014b). It should be noted that a key step in the synthesis process of nanocomposite is symmetrical placement of the photocatalytic shell on the corresponding core. This step is implemented using techniques such as hydrothermal and solvothermal method (Li et al. 2015; Vanga et al. 2015), sol-gel autocombustion method (Bhukal et al. 2014), calcination (Huang et al. 2015b), and in situ precipitation method (Chen et al. 2015). Informed by this fact, various morphologies with different symmetries have been achieved for the core-shell magnetic nanophotocatalysts.

In the case of heterojunction magnetic photocatalysts, the tight coupling of magnetic and photocatalytic components, as the major reason of structural stability and the emergence of synergistic effects, is of paramount importance. Researchers have employed various methods for synthesizing heterojunctions such as wet chemical process (Hankare et al. 2011), hydrolysis combining solvent evaporation method (Yu et al. 2015), precipitation method (Cao et al. 2015c), sol-gel method (Xu et al. 2009), electrospinning technique (Wang et al. 2014), and hydrothermal process followed by a polymerization method (Leng et al. 2013b).

In regard to the bonding between components, there are two major approaches to the synthesis of hybrid nanostructures: surface assembly and in situ growth. In the surface assembly approach, components are separately synthesized and then the final hybrid structure is obtained by distributing each

Table 1 Various magnetic visible light photocatalysts used to purify different organic contaminants

Type of catalyst	Morphology	Contaminants	Irradiation time (min)	Degradation efficiency	No. of recycle runs	References
Fe_3O_4/WO_3	Core-shell	Methylene blue (MB), rhodamine B (RhB)	120	> 90%	4 cycles	Xi et al. 2011
Ce/mesoporous TiO_2/Fe3O_4	Core-shell	MB	360	> 90%	4 cycles	Zhongliang et al. 2012
Fe_3O_4@SiO_2@AgCl:Ag	Core-shell	RhB	4	About 100%	8 cycles	An et al. 2012
Fe_3O_4@SiO_2@Ag_3PO_4	Core-shell	RhB	45	Nearly 100%	5 cycles	Yao et al. 2014b
γ-Fe_2O_3/ZnO	Core-shell	MB, RhB, Methyl orange (MO)	50	95.2%	6 cycles	Liu et al. 2012a
Fe_3O_4@Cu_2O/Cu	Core-shell	MO	20	96%	5 cycles	Wang et al. 2013
Fe_3O_4@TiO_2@Au	Core-shell	4-Nitrophenol	3	100%	10 cycles	Zhou et al. 2015
$CoFe_2O_4/SiO_2/TiO_2$	Core-shell	Dichlorophenol-indophenol	4	87.27%	–	Hamad et al. 2015
Polyaniline-modified $CoFe_2O_4$-TiO_2	Heterojunction	MB	160	Nearly 50%	5 cycles	Leng et al. 2013b
Fe_3O_4/AgBr	Heterojunction	MO	12	85%	3 cycles	Cao et al. 2015c
$TiO_2/ZnFe_2O_4$	Heterojunction	MO	240	35%	–	Xu et al. 2009
TiO_2-Al_2O_3-$ZnFe_2O_4$	Heterojunction	Methyl red, Thymol blue	15	70–80%	–	Hankare et al. 2011
Fe_3O_4@TiO_2/CdS	Heterojunction	RhB	120	97.65%	3 cycles	Wang et al. 2014

component in a suitable solvent and mixing the solutions under controlled conditions. This method, however, has a number of disadvantages such as formation of large and irregular particles and weak bonding between components. In the in situ growth approach, the nuclei of one component grow on the other component, providing a stronger junction between components, as well as a regular distributed structure (Yan et al. 2013). Accordingly, most nanoheterostructure photocatalysts have been synthesized based on in situ growth technique and high performance and stability have been exhibited, which can be attributed to strong bonding of components in the in situ growth hybridization.

Magnetic-nanophotocatalyst-based core-shell structure

Magnetic core-shell nanostructures comprise a large group of nanocomposites, with a broad range of applications such as catalysis (Chen et al. 2011; Kong et al. 2016; Zhang et al. 2013), photocatalysis (Jang et al. 2014; Liu et al. 2012a; Xi et al. 2011), and adsorption (Bayal and Jeevanandam 2013; Tanhaei et al. 2016; Zhang et al. 2016). Given the interaction between core and shell layers and thus improved optical properties of composite along with easy recovery via an external magnetic field, these structures have been highly popular as a photocatalyst (Liu et al. 2012a). The simplest type of these composites is made of a core and a shell, each with a specific role in photocatalytic application.

Using a multistep approach, Liu et al. fabricated γ-Fe_2O_3/ZnO nest-like hollow nanocomposites, as shown in Scheme 1. First, colloidal carbon spheres were covered with a layer of FeS_x in the presence of thioacetamide (TAA) and the sandwiched nanostructures of CS/FeS_X/ZnO were produced by reflux at 170 °C for 60 min. Then, γ-Fe_2O_3/ZnO nest-like hollow nanostructures were obtained by calcination of composites at 500 °C for 2 h.

The photocatalytic application of the magnetic γ-Fe_2O_3/ZnO structures was investigated by the degradation of organic dyes including MB, RhB, and MO under irradiation of a Xe lamp (500 W) with a cutoff filter of 420 nm.

The degradation efficiencies for MB, RhB, and MO in the presence of γ-Fe_2O_3/ZnO nest-like hollow nanocomposites were 95.2, 91.1, and 82.5%, respectively. In the commercial ZnO nanoparticles, these values were 87.6, 51.5, and 39.5%, respectively. The enhancement of photoactivity in the case of γ-Fe_2O_3/ZnO nest-like hollow nanostructures is mostly due to the synergetic effects between the two semiconductors with varying energy levels. It was suggested that Fe_2O_3 accepted electrons in the CB of ZnO, so Fe (III) was reduced to Fe (II) and electron-hole recombination was suppressed effectively (Liu et al. 2012a).

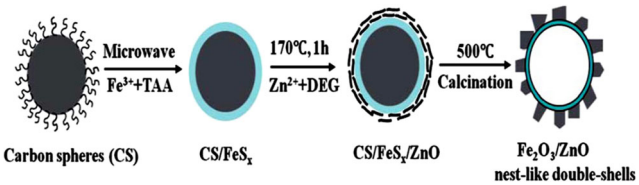

Scheme 1 Schematic illustration of the synthesis steps of γ-Fe_2O_3/ZnO nest-like hollow nanocomposites (Liu et al. 2012a)

Jang et al. fabricated ferromagnetic TiO_2-Fe_2O_3 core-shell nanostructures by a sol-gel procedure using cetyltrimethyl ammonium bromide (CTAB) as the controlling size agent. They prepared this nanostructure with various concentrations of Fe salt, finding that the magnetic nanophotocatalyst with lower concentration of Fe displayed optimal photocatalytic performance and degraded MB by 90% after 200 min under room light irradiation in the presence of H_2O_2. The enhanced photocatalytic activity of TiO_2-Fe_2O_3 core-shell nanostructures was due to the synergetic effects of TiO_2 core and Fe_2O_3 shell (Jang et al. 2014).

Fe_3O_4/WO_3 hierarchical core-shell structures were synthesized by Xi et al. (2011). Fe_3O_4 microspheres play the role of a charge collector and inhibit the recombination of photoexcited electrons and holes. The Fe_3O_4/WO_3 nanocomposite was prepared using a solvothermal approach followed by calcination at 420 °C for 30 min. According to authors, the photocatalytic activity of magnetic Fe_3O_4/WO_3 nanostructures could be attributed to the following factors: (1) high surface area of Fe_3O_4/WO_3 nanocomposites (34 m^2 g^{-1}), which provides more active sites for photocatalytic degradation and (2) high conductivity of Fe_3O_4. The microspheres and synergistic effects between Fe_3O_4 core and WO_3 shell are shown in Scheme 2. They claimed that lower conduction bond (CB) of Fe_3O_4 compared to WO_3 led to the migration of photoexcited electrons from CB of WO_3 to CB of Fe_3O_4, which enhanced photodegradation of MB. Finally, electrons collected

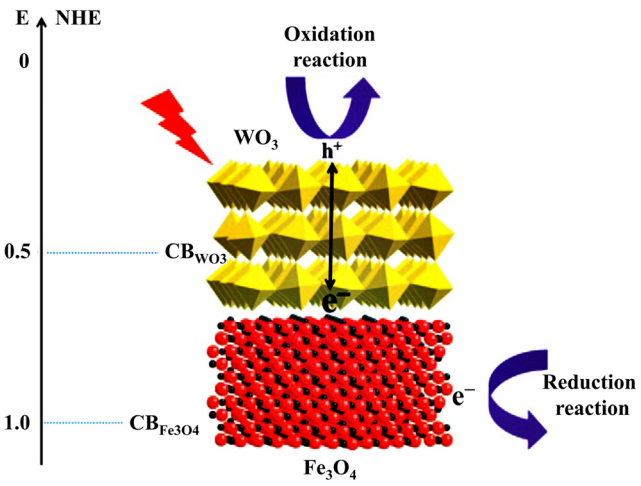

Scheme 2 Illustration of charge transfer in magnetic Fe_3O_4/WO_3 core-shell nanocomposites (Xi et al. 2011).

by Fe_3O_4 could be reduced by dissolved O_2 in the solution (Xi et al. 2011).

As mentioned in the last section, metal ion doping is a suitable method to improve the photocatalytic activity of magnetic nanocomposites. Different magnetic ion-doped photocatalysts with core-shell nanostructure have been fabricated using metal ions such as Au (Zhou et al. 2015), Ce (Zhongliang et al. 2012), and Ho (Shi et al. 2011) and applied as efficient photocatalysts under visible light irradiation.

In a procedure involving surface modification of Fe_3O_4@TiO_2 microspheres, Zhou et al. (2015) prepared multifunctional Au decorated Fe_3O_4@TiO_2 nanocomposites. SEM and TEM images of Fe_3O_4@TiO_2@Au microspheres are shown in Fig. 4, which confirm grafted Au nanoparticles on the surface of Fe_3O_4@TiO_2 microspheres.

The photoactivity of fabricated nanocomposites in reducing 4-nitrophenol (4-NP) to 4-aminophenol (4-AP) in the presence of $NaBH_4$ under visible light was evaluated. According to the results, Fe_3O_4@TiO_2@Au microspheres were able to reduce 4-NP to 4-AP after 3 min. It was found that the reduction of 4-NP followed the modified Langmuir-Hinshelwood model, and the pseudo-first-order rate constants with illumination and dark were equal to 1.18 and 0.421 min^{-1}, respectively (Zhou et al. 2015).

A cerium-doped mesoporous titanium dioxide-coated magnetite (Ce/$MTiO_2$/Fe_3O_4) core-shell structure was fabricated by the hydrolysis of tetrabutyltitanate (TBT) with precursors of ammonium ceric nitrate and TBT in the presence of Fe_3O_4 particles using a vacuum rotary evaporator and calcination at 500 °C (Zhongliang et al. 2012). The photocatalytic activity of Ce/$MTiO_2$/Fe_3O_4 under visible light degradation was evaluated on the MB solution (50 ppm) with 0.5-mol% Ce/$MTiO_2$/Fe_3O_4 exhibiting the highest photoactivity. UV-Vis DRS analysis showed that the presence of cerium led to a red shift in the adsorption profile, so that the Ce doping improved the photo-utilization of $MTiO_2$/Fe_3O_4 and generated more electron-hole pairs under photo-irradiation. However, to identify the magnetic properties of nanocomposites, no characterization analysis was performed (Zhongliang et al. 2012).

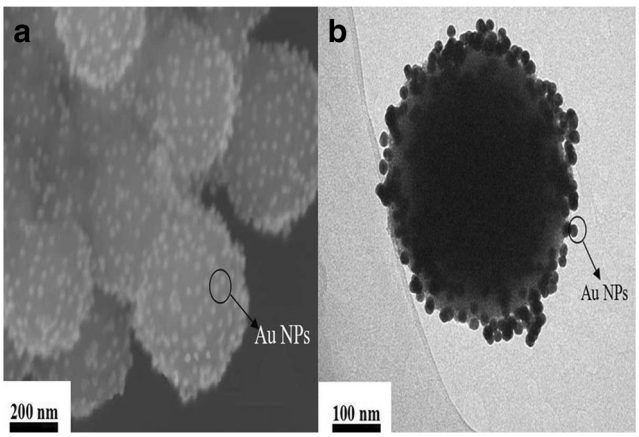

Fig. 4 **a** SEM image and **b** TEM image of Au decorated Fe_3O_4@TiO_2 magnetic microspheres (Zhou et al. 2015)

Holmium (Ho) was used as a doping agent in the synthesis of Ho/TiO_2/Fe_3O_4 using CTAB and *n*-pentanol as the surfactant and cyclohexane as the oil phase (Shi et al. 2011). This magnetic photocatalyst was used for the degradation of MO under 300-W metal halide lamp for 10 h. It was suggested that the presence of Ho ions on the TiO_2/Fe_3O_4 nanoparticles affected the electron-hole recombination rate according to the following equations:

$$Ho^{3+} + e^- \rightarrow Ho^{2+} \quad (2)$$

$$Ho^{2+} + O_2 \rightarrow O_2^{\cdot -} + Ho^{3+} \quad (3)$$

Thus, Ho sites on the TiO_2/Fe_3O_4 nanoparticles trapped the photo-excited electrons and increased the photocatalytic activity. However, the results suggested that the optimum amount of Ho doping was 20%. The higher amount of Ho made the dopants into the recombination centers of the excited electrons and reduced the photocatalytic activity (Shi et al. 2011).

In recent years, magnetic core-shell nanostructures including silver halides (AgX, X = Cl, Br) have gained considerable attention due to small band gap of silver halides. Furthermore, the presence of metallic silver on silver halides improves their ability for the absorption of visible light irradiation by the surface plasmon resonance effect (Huang et al. 2015a; Shekofteh-Gohari and Habibi-Yangjeh 2015).

Fe_3O_4@ZnO/AgCl (1:10) was fabricated by a simple large-scale method at low temperature (96 °C) in water (Shekofteh-Gohari and Habibi-Yangjeh 2015). This nanocomposite showed that the first-order degradation rate constant of RhB was 35 times higher than that of the Fe_3O_4@ZnO nanocomposite. It was demonstrated that Fe_3O_4@ZnO/AgCl nanocomposites exhibited higher visible light absorption efficiency. Thus, the nanocomposites exhibit increased photocatalytic activity under visible light irradiation caused by the generation of more electron-hole pairs.

In another research, Huang et al. prepared magnetic core-shell structured Ag/AgBr@Fe_2O_3 composite via a facile hydrothermal method. In the synthesized samples, different mass fractions of Fe_2O_3 in the total weight of Fe_2O_3 and $AgNO_3$ were 1, 3, 5, and 10% (Huang et al. 2015a).

Ag/AgBr@Fe_2O_3 nanostructures showed antibacterial properties and improved photocatalytic activity for the degradation of organic pollutants under visible light irradiation. The authors stated that enhancement of catalytic activity of 3% Ag/AgBr@Fe_2O_3 could be attributed to the synergistic effect of AgBr and Fe_2O_3, which could improve the formation of reactive species and thus improve the photocatalytic performance. The proposed mechanism of the reaction process for nanocomposites has been depicted in Scheme 3.

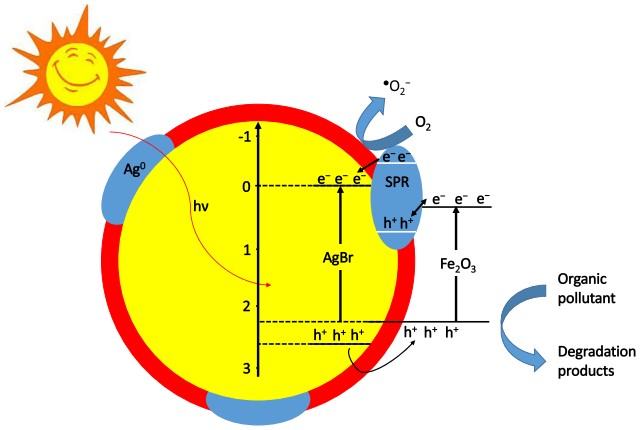

Scheme 3 Suggested mechanism for the photocatalytic degradation of MO under visible light irradiation (Huang et al. 2015a)

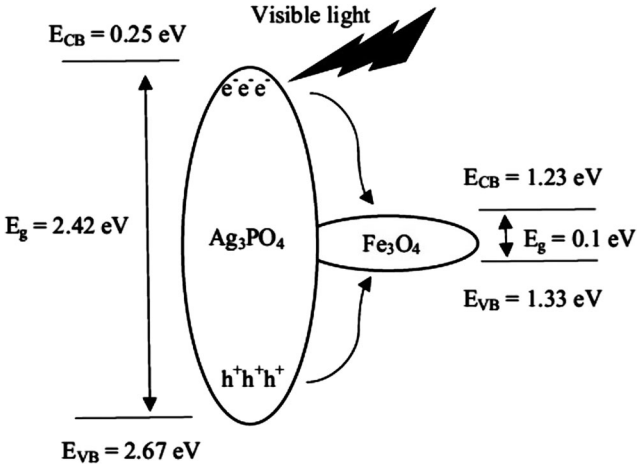

Fig. 5 Mechanism of migration of photo-excited charges on magnetic Fe_3O_4 (Yao et al. 2014a)

As shown in Scheme 3, Fe_2O_3 created numerous active sites for adsorption of organic pollutants, and the interactions of Fe_2O_3, AgBr, and metallic Ag nanoparticles inhibited the recombination of photo-excited electron-hole pairs and thus enhanced the photocatalytic activity. It was suggested that Ag nanoparticles absorbed light and produced electron-hole pairs. Then, photo-excited electrons migrated to the CB of AgBr and reduced the dissolved O_2 in the solution to the superoxide radical. Beside, because of the Schottky barrier at the metal-semiconductor interface, the excited electrons on the Fe_2O_3 were combined with holes on the Ag nanoparticles. On the other hand, the holes on the VB of AgBr were transferred to the VB of Fe_2O_3 and oxidized the adsorbed organic pollutants on the layer of Fe_2O_3 (Huang et al. 2015a).

Some researchers have proposed that in a magnetic-semiconductor nanophotocatalytic such as $Fe_3O_4@SiO_2@Ag_3PO_4$ (Yao et al. 2014a), $Fe_3O_4@SiO_2@Co_3O_4$ (Wang et al. 2015), $MgFe_2O_4@SiO_2@Ag_4SiW_{12}O_{40}/Ag$ (Tang et al. 2014), and $CoFe_2O_4/SiO_2/TiO_2$ (Hamad et al. 2015), direct combination with magnetic core and photocatalytic shell generates a quenching effect that deteriorates the photocatalytic performance (Yao et al. 2014a). It has been established that the presence of the SiO_2 interlayer reduces the quenching effect and protects the magnetic core from chemical corrosion (Yao et al. 2014a).

Yao et al. prepared core-shell magnetic nanocomposites of $Fe_3O_4@SiO_2@Ag_3PO_4$ by a facile precipitation method with a grain size ranging from 200 to 400 nm (Yao et al. 2014a). The photocatalytic activity of Ag_3PO_4, $Fe_3O_4@Ag_3PO_4$, and $Fe_3O_4@SiO_2@Ag_3PO_4$ was investigated for the degradation of RhB under visible light irradiation for 45 min. Results showed that the photocatalytic activity of $Fe_3O_4@SiO_2@Ag_3PO_4$ was close to that of pure Ag_3PO_4. On the other hand, the photocatalytic activity of $Fe_3O_4@Ag_3PO_4$ was extremely low. In fact, Fe_3O_4 acted as a recombination center and photo-excited charges were injected from Ag_3PO_4 into Fe_3O_4, as shown in Fig. 5.

A yolk-shell $Fe_3O_4@SiO_2@Co_3O_4$ nanostructure was fabricated by a three-step procedure using urea and a mixed solution containing water and ethanol (9:1). The synthesized nanostructures were used for photocatalytic oxidation of water to oxygen in the $Ru(bpy)_3^{2+}$–$S_2O_8^{2-}$ (bpy = 2, 2′-bipyridine) system. It is noteworthy that bpy and $S_2O_8^{2-}$ act as photosensitizer and oxidizing agent, respectively (Wang et al. 2015).

Tang et al. synthesized magnesium ferrite nanoparticles (MFNs) by a hydrothermal method and used them as magnetic core for the synthesis of ferromagnetic $MFNs@SiO_2/Ag_4SiW_{12}O_{40}/Ag$ photocatalyst. For Ag@silver-based salt photocatalysts, the presence of anions with higher charges yielded stronger photocatalytic capability; thus, $SiW_{12}O_{40}^{4-}$ was applied as anion (Tang et al. 2014).

Photocatalytic activity of nanocomposites was investigated in the degradation of MB and disinfection of *E. coli* bacteria. It was found that $MFNs@SiO_2/Ag_4SiW_{12}O_{40}/Ag$ photocatalyst synthesized under 4-h UV irradiation demonstrated the optimal performance. It was assumed that the localized surface plasmon resonance (LSPR) effect of Ag NPs on the surface of $Ag_4SiW_{12}O_{40}$ could improve its light absorption in the visible light region and therefore promote the photocatalytic performance of magnetic nanostructure. Basically, Ag NPs suppress the recombination of photo-excited charges in $Ag_4SiW_{12}O_{40}$ by acting as an electron trapping agent (Tang et al. 2014).

In another study, a core/shell/shell spherical nanostructure, $CoFe_2O_4/SiO_2/TiO_2$, with a proper saturation magnetization ($M_s = 6.53$ emu g^{-1}), was synthesized by sol-gel hydrolysis and condensation of titanium isopropoxide ($C_{12}H_{28}O_4Ti$) followed by calcination treatment at 300 °C. As in previous cases, SiO_2 layer acted as a barrier layer between the magnetic core and the photoactive shell and inhibited the $CoFe_2O_4$ tendency to recombine photo-excited electrons and holes. The authors declared that direct contact between TiO_2 and iron oxide could cause problems such as photodissolution of iron

oxide, stimulation of electron-hole recombination, and aggregation of magnetic photocatalytic particles (Hamad et al. 2015).

Magnetic-nanophotocatalyst-based heterojunction structure

Magnetic heterojunction nanostructures are effective photocatalysts that utilize the suitable properties of their components. Like core-shell structures, the magnetic part of heterojunction provides a separable heterostructure and simple recovery of catalyst. Moreover, synergetic effects are considered in heterojunction structures (Leng et al. 2013a; Shojaei et al. 2015).

The p-n junction is the most common type of heterojunction structure in the magnetic photocatalysts (Cao et al. 2014b, 2015b; Hankare et al. 2011). Magnetic p-n junction is formed by bringing n-type (magnetic part such as Fe_3O_4) and p-type (photocatalytic part) semiconductors into close contact, as shown in Fig. 6. An electric field is formed between the positive ion cores in the n-type semiconductor and negative ion cores in the p-type semiconductor (Cao et al. 2014a, b). The contact of n-type semiconductor with p-type semiconductor leads to diffusion of excess electrons of the n-type semiconductor to the p-type and migration of excess holes from the p-type semiconductor to the n-type one. As a result, the recombination of photo-excited electrons and holes is inhibited and photocatalytic performance of photocatalyst is amplified (Cao et al. 2014b, 2015b).

As TiO_2 is the key compound in the photocatalytic area, different structures of TiO_2 has been used in the synthesis of magnetic-nanophotocatalyst-based heterojunction structures such as nanostructures (Sathishkumar et al. 2013), microspheres (Leng et al. 2013a; Tang et al. 2013), nanofibers (Wang et al. 2014), and hollow bowls (Mou et al. 2012).

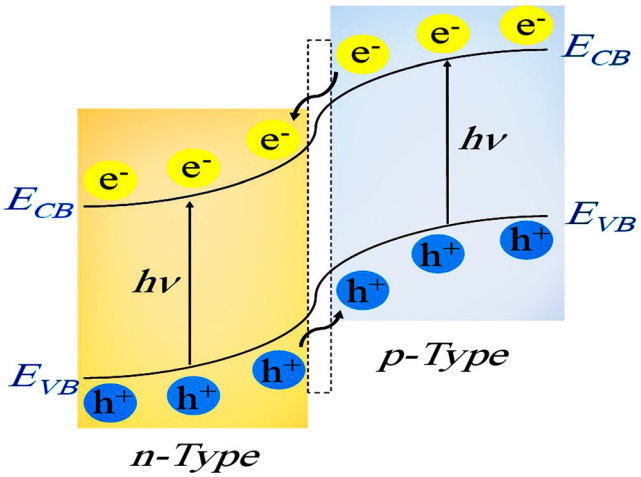

Fig. 6 The energy band structure and the movement of electrons and holes in a p-n heterojunction

By combining hydrothermal and co-precipitation techniques, a novel type of hierarchically magnetic K-OMS-2/TiO_2/Fe_3O_4 heterojunction (K-OMS: cryptomelane-type manganese oxide) was successfully synthesized using manganese oxide nanowires (K-OMS-2) and TiO_2 nanoparticles. The as-prepared nanocomposites revealed high magnetic response and great degradation efficiency (85.7%) for humic acid under simulated solar irradiation. The desirable photocatalytic performance of K-OMS-2/TiO_2/Fe_3O_4 heterojunctions was ascribed to the important role of manganese oxide nanowires. Actually, as a dispersing template, the K-OMS-2 reduced the size of TiO_2 to nanoscale during the synthesis process and therefore the specific surface area of the fabricated nanocomposites was increased. This could lead to the synthesis of materials with higher photocatalytic activity. Furthermore, it was claimed that the Mn^{3+}/Mn^{4+} in the synthesized heterojunctions had a direct effect on the electron transfer and inhibited the recombination of electron and hole pairs (Zhang et al. 2012).

Wang et al. used TiO_2 nanofibers for the synthesis of Fe_3O_4@TiO_2/CdS heterostructures. The electrospinning technique was applied to prepare the Fe_3O_4-embedded TiO_2 (Fe_3O_4@TiO_2) magnetic nanofibers and Fe_3O_4@TiO_2/CdS heterostructures were obtained by a hydrothermal process. TEM images of as-synthesized nanocomposites are presented in Fig. 7, which confirm the uniform dispersion of Fe_3O_4 and CdS nanoparticles on the surface of TiO_2 nanofibers (Wang et al. 2014).

The Fe_3O_4@TiO_2/CdS multifunctional photocatalysts exhibited high efficiency in the degradation of RhB under UV, visible, and sunlight irradiation. The CdS nanoparticles did not have any significant effect on improving the photocatalytic performance of nanocomposites under UV irradiation. This can be attributed to the lack of photo-excitation of CdS under UV irradiation and the TiO_2 nanofibers were the only source of photocatalytic activity. However, under the visible and

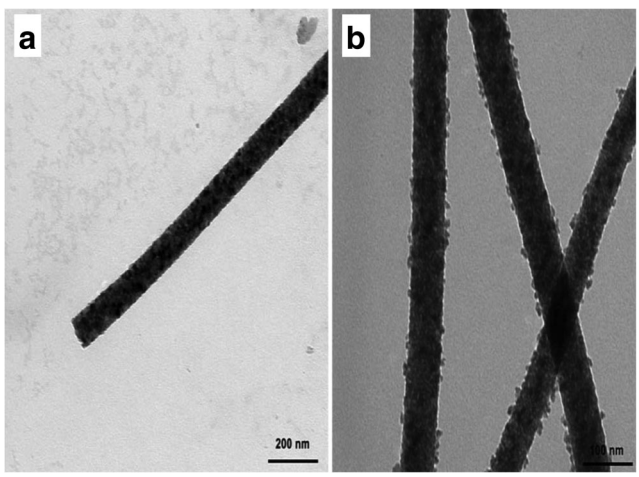

Fig. 7 TEM image of **a** Fe_3O_4@TiO_2 nanofibers and **b** Fe_3O_4@TiO_2/CdS heterostructures (Wang et al. 2014)

simulated sunlight irradiation, anatase TiO_2 nanofibers were unable to exhibit photocatalytic performance and the photocatalytic activity was derived from the CdS nanoparticles (Wang et al. 2014).

Magnetic γ-Fe_2O_3/TiO_2 hollow bowls were prepared by a simple combined process including the side-by-side electrospray method with a non-equilibrium calcination process. As shown in Fig. 8a, SEM images have the typical bowl-shaped structure of as-synthesized heterostructures with rough surfaces and small holes of 10 nm on them.

Moreover, it was maintained that a Fe^{3+}-doped-TiO_2 transition layer was formed between the γ-Fe_2O_3 and TiO_2 phases, as presented in Fig. 8b. The incorporation of Fe^{3+}-doped-TiO_2 transition layer between the γ-Fe_2O_3 and TiO_2 layers could foster the separation of photo-excited electron-hole pairs and it was the main reason for the enhanced photocatalytic performance of γ-Fe_2O_3/TiO_2 hollow bowls compared to the pure γ-Fe_2O_3, for decolorization of RhB under the visible light irradiation (Mou et al. 2012).

It is clear that the preparation condition of magnetic heterojunctions directly influences the crystalline phase of photocatalyst and plays an important role in the synthesis of these structures. In another research, it was found that co-precipitated $CoFe_2O_4$ enhanced the formation of $CoFe_2O_4$/TiO_2 nanocatalysts and the calcination process at 400 °C led to the phase conversion of TiO_2 from anatase to rutile. The XRD analysis of the as-prepared $CoFe_2O_4$/TiO_2 heterojunction nanostructures revealed that the conversion of anatase to rutile phase of TiO_2 was the most important reason for enhanced photocatalytic properties. In fact, the rutile phase of TiO_2 (3.0 eV) is excited by visible light to produce the photo-excited charges and radicals, whereas anatase phase of TiO_2 (3.2 eV) demands higher energy for excitation and generation of electron-hole pairs. Subsequently, the phase conversion leads to the activation of synthesized $CoFe_2O_4$/TiO_2 nanostructures under visible light irradiation (Sathishkumar et al. 2013).

Using carbon spheres as the template and urea as the precipitation agent, α-Fe_2O_3/TiO_2 heterostructure hollow spheres was fabricated and used for photocatalytic degradation of RhB under visible light. The hollow α-Fe_2O_3/TiO_2 structures revealed a relatively high surface area (31.8 m^2 g^{-1}). The effect of some synthesis parameters was evaluated on photocatalytic performance of heterojunction nanostructures, such as calcination temperature and the molar ratio of titanium to iron (*R*). It was found that the optimum value of calcination temperature and *R* was equal to 400 °C and 2:1.5, respectively. At this optimum condition, the as-synthesized α-Fe_2O_3/TiO_2 heterostructures exhibited 98% efficiency for decolorization of RhB (Tang et al. 2013).

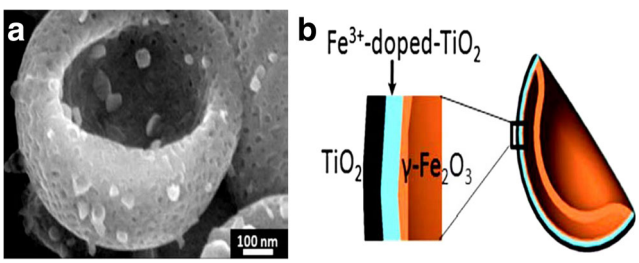

Fig. 8 **a** SEM image and **b** schematic layered structure of the as-prepared bowl shaped γ-Fe_2O_3/TiO_2 nanostructures (Mou et al. 2012)

With the exception of TiO_2, some other semiconductors are used in the structure of magnetic nanostructures, such as Ag_2O and ZnO (Cai et al. 2015), Cu_2O (Cao et al. 2015a), and WO_3 (Shojaei et al. 2015). The heterojunction structures synthesized with these semiconductors exhibited efficient visible light photocatalytic activity and convenient magnetic properties with great potentials for water purification.

Hierarchical Ag_2O-ZnO-Fe_3O_4 visible light photocatalysts were prepared by a low-temperature hydrothermal method (130 °C) with different mass ratios of Ag_2O and ZnO. The photocatalytic performance of the as-synthesized samples was evaluated for the degradation of RhB and $(Ag_2O)_{0.6}$-ZnO-Fe_3O_4 showed the highest photocatalytic efficiency (98.5%). The enhancement of the photocatalytic activity was ascribed to the inhibition of electron-hole recombination on the surface of $(Ag_2O)_{0.6}$-ZnO-Fe_3O_4 nanostructures (Cai et al. 2015).

Cao et al. fabricated superparamagnetic Cu_2O/chitosan-Fe_3O_4 heterojunction nanocomposites by a facile one-step precipitation-reduction process using a magnetic chitosan chelating copper ions as the precursor. It has been shown that Cu_2O wrapped in the chitosan matrix embedded with Fe_3O_4 nanoparticles, and consequently Cu_2O/chitosan-Fe_3O_4 nanostructures provided a relatively large specific surface area (28.6 m^2 g^{-1}) and special di-modal pore structure. Moreover, the photocatalytic activity of nanophotocatalysts was examined by decolorization of reactive brilliant red X-3B (X-3B) under visible light irradiation and the dye X-3B was almost completely decolorized after 60-min irradiation in the presence of 1.0-g/L Cu_2O/chitosan-Fe_3O_4 nanocomposites for 50-mg/L X-3B solution at pH 5.6. The Cu_2O/chitosan-Fe_3O_4 nanostructures revealed a high reusability and stability performance on decolorization of X-3B in a way that the decolorization efficiency of the first to the fifth runs was 99.8, 97.2, 91.5, 88.4, and 87.4%, respectively (Cao et al. 2015a).

WO_3/TiO_2/Fe_3O_4 nanomagnetic particles with different amounts of WO_3 content (1, 3, 5, 8, and 10 wt%) were synthesized by the sol-gel method and used as reusable photocatalyst for the removal of direct blue 71 from aqueous solution. The nanostructures synthesized with 5%WO_3 showed enhanced photocatalytic performance under the visible light irradiation compared with the pure TiO_2, TiO_2/Fe_3O_4, and 5%WO_3/TiO_2 nanoparticles. Superparamagnetic microspheres of 5%WO_3/TiO_2/Fe_3O_4 with a saturation magnetization equal to 18.2 emu g^{-1} could be easily separated from

aqueous solutions with a magnet and about 85% activity of recycled photocatalysts remained after 5 cycles.

The enhanced photocatalytic performance of 5%WO_3/TiO_2/Fe_3O_4 nanocomposites was attributed to the synergistic interactions between WO_3 and TiO_2 and the electron-hole separation and transformation, as shown in Scheme 4.

In fact, the interaction of WO_3 and TiO_2 and the positive potential of CB of WO_3 compared to TiO_2 increased the lifetime of the photogenerated electrons and holes and thus the efficiency of photocatalytic degradation of dye promotes (Shojaei et al. 2015).

Scaling up the solar light photocatalytic systems

Industrial and real applications of solar light photocatalysts

To date, various real applications of heterogeneous photocatalysis have been reported by many researchers, most of which are associated with capability of photocatalysts in water and air matrices disinfection and inactivation of microorganisms. It is well known that the most commonly used photocatalyst is TiO_2, which is a non-toxic, chemically stable, and low-cost material. The most common real-life applications of TiO_2 include air purification (Goswami et al. 1997), medical and biological applications (Shiraishi et al. 2009), laboratory and hospital waste purification (Yu et al. 2003), food and pharmaceutical industries (Yu et al. 2003), hydrogen production through splitting of water (Ni et al. 2007), and wastewater treatment (Mahmoodi and Sargolzaei 2014a,b).

However, due to some operational limitations such as wide band gap and fast recombination of electron-hole pair, TiO_2 is no longer an ideal photocatalyst and researchers are looking for alternatives (Mahmoodi et al. 2017).

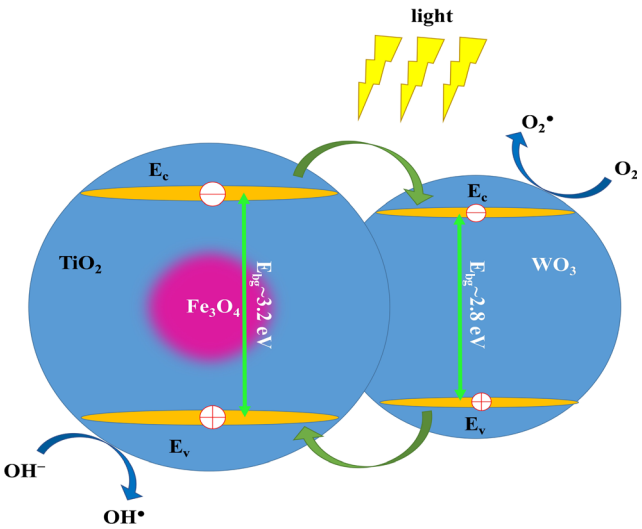

Scheme 4 Proposed mechanism for photocatalytic degradation of direct blue dye using 5%WO_3/TiO_2/Fe_3O_4 nanostructures (Shojaei et al. 2015)

Solar-light photocatalysts have been claimed to offer a good alternative to TiO_2 in real-life applications. Many researchers have used these materials for practical purposes at pilot-plant scale in areas such as hydrogen production (Salgado et al. 2016; Villa et al. 2013), photocatalytic treatment of pesticides (Oller et al. 2006; Spasiano et al. 2013), oxidation of organic compounds (Spasiano et al. 2013), and degradation of organic wastewater (Shaban et al. 2016). For instance, two different photocatalytic systems, one based on a Pt/ (nitrogen doped TiO_2) and the other based on a Pt/CdSe-ZnS composite, were used for the simultaneous photocatalytic hydrogen production and organic pollutant removal using a pilot-plant solar reactor equipped with a compound parabolic collector (CPC). Aqueous solutions of formic acid and glycerol were prepared as the synthetic wastewater, and municipal wastewater from the Sewage Treatment Plant of Almeria (Spain) was used as the real wastewater. The highest energy efficiency (2.5%) was achieved when using Pt/(TiO_2-N) in a 0.05-M formic acid aqueous solution after 5-h exposure to the sunlight irradiation. Even though the real wastewater experiments produced smaller amounts of hydrogen, the possible use of municipal wastewaters for photocatalytic generation of hydrogen at large scale was demonstrated (Villa et al. 2013).

Also, TiO_2/Cu(II) photocatalyst was used to exhibit the possibility of converting benzyl alcohol to benzaldehyde in a aqueous solution under natural solar radiation at pilot-plant scale. The initial cupric ion concentration, incident solar irradiance, and temperature were the main operational parameters affecting the benzyl alcohol oxidation rate. The possibility of cupric species regeneration (as catalyst) was shown by air or oxygen bubbling into the pilot-plant in dark conditions (Spasiano et al. 2013). Table 2 presents some visible light photocatalysts, which are practically used in different areas at pilot-plant scale.

Since the stability, easy separation, and regeneration of photocatalyst are key parameters in industrial scale application, recently, researchers have paid special attention to magnetic visible light photocatalysts, which could be easily separated from the reaction medium by applying an external magnetic field. However, the practical use of magnetic photocatalysts at industrial scale has not yet been reported, which could be due to the low synthesis efficiency of these materials.

Economic aspects of the solar-light-based processes

It is well-known that economics of operational processes has a significant effect on their commercial justification. As far as authors are concerned, few studies have addressed the economic considerations of solar light-based photocatalytic

Table 2 Various solar-light photocatalysts practically used in different areas at pilot-plant scale

Type of photocatalyst	Field of use	Efficiency	Substance	Type of reactor	References
TiO_2/Cu(II)	Oxidation of benzyl alcohol	53.3%	Benzaldehyde	Solar CPC reactor	Spasiano et al. 2013
TiO_2 (Degussa P-25)	Degradation of hazardous water-soluble pesticides	80–90%	Cymoxanil, Methomyl, Oxamyl, Dimethoate, Pyrimethanil and Telone	Solar CPC reactor	Oller et al. 2006
Carbon-modified TiO_2	Degradation of polychlorinated biphenyls	92–95%	Clean seawater	Solar falling film reactor	Shaban et al. 2016
Au/TiO_2	Hydrogen production	1.8–2.9%	Alcohols, organic acids, municipal wastewater, industrial wastewater	Solar CPC reactor	Salgado et al. 2016
Pt/(TiO_2-N) Pt/CdSe-ZnS	Hydrogen production	2.5%	Formic acid, Glycerol, municipal wastewater	Solar CPC reactor	Villa et al. 2013

processes. Researchers have reported that the most important factor in the economic prediction of solar light-based processes is the cost of fabrication and maintenance of the reactor, and the accurate calculation of the required reactor area (under illumination) is a fundamental parameter in the accurate prediction of economic calculations. For instance, Turchi and Link claimed that non-concentrating solar light reactors could increase the economic justification of solar light-based processes compared to other processes such as activated carbon adsorption and UV/H_2O_2 photolysis (Link and Turchi 1991). Also, Goswami claimed that the cost of visible light photocatalytic process varies from 0.53 to 2.5 ($\$ m^{-3}$) depending on the type of process (Goswami 1997). It should be noted that with the exception of the photocatalytic reactor, some other factors such as type of wastewater, mode operation, and location of plant directly affect the cost prediction.

Toxicity of treated water

The toxicity of treated water by the magnetic photocatalysts could emerge from the main causes: (1) the incomplete photodegradation of organic molecules and the production of intermediates and (2) the remaining of magnetic photocatalysts in the treated water due to the lack of full separation of nanophotocatalysts. In the former case, the theory of photocatalytic processes states that at the end of process, the persistent organic pollutants transform to the safe compounds such as CO_2 and H_2O (Cao et al. 2014b), while many researches have shown that what really happens in the photocatalytic treatment process is that organic compounds containing a large number of benzene rings are broken down into several smaller intermediates. Usually, produced intermediates are identified using mass spectroscopic techniques, e.g., GC-MS or LC-MS spectroscopy. For instance, the produced intermediates of naphthalene degradation in aqueous suspension of TiO_2 under UV irradiation were studied using GC-MS spectroscopy and 15 different compounds were identified (Theurich et al. 1997). Also, in our previous research, we found that photocatalytic degradation of reactive blue 19 dye on the surface of BiOI nanoparticles under natural sunlight irradiation generates several smaller molecules such as indoline, coumarin, and dihydroxanthin (Mahmoodi et al. 2017).

In the latter case, if magnetic photocatalyst is separated from the treated water by applying a relatively weak magnetic field or magnetic component does not have a high magnetic property, it is possible that part of the photocatalyst remains in the treated water. Many researches have focused on toxicity of magnetic nanoparticles and found that the toxicity of magnetic particles depends on several parameters including chemical composition, dose, size, structure, solubility, surface chemistry, and structure of the magnetic nanoparticles (Markides et al. 2012; Reddy et al. 2012). However, the effect of these nanomaterials has been largely studied in vitro conditions but long-term in vivo researches have not been carried out extensively (Markides et al. 2012). Finally, it cannot be argued that the wastewater treated by magnetic nanophotocatalysts is free from any toxicity and can be used as drinking water. What we can say is that after purification with the photocatalytic process, it is possible to release treated wastewater to surface waters or further refine it by the commonly used wastewater treatment methods (Franquet-Griell et al. 2017).

Summary and perspectives

The unique photocatalytic properties of narrow-band gap semiconductors have attracted increasing attention for researcher. Photocatalytic degradation of toxic organic pollutants in wastewater with these photocatalysts provides many advantages, such as high degradation efficiency, utilization of free solar energy, and low-cost operation. A variety of types, structures, and preparation methods for visible light photocatalysts have been reported. However, the problem of separation and recovery from solution is one of the main challenges in application of these structures and industrialization of photocatalytic processes.

Magnetic heterogeneous photocatalysts can provide a solution for this problem in which a component with magnetic properties (such as Fe_2O_3, Fe_3O_4, and $CoFe_2O_4$) is incorporated in the structure of hybrid photocatalyst. The structure of magnetic-semiconductor nanocomposite heterostructure can be simply divided into core-shell, matrix-dispersed, Janus, and shell-core-shell structures. Many researches have been undertaken for the synthesis, characterization, applications, and mechanisms of visible light magnetic heterostructure photocatalysts. To promote the photocatalytic performance of magnetic photocatalysts, a bulk of studies has explored their composition, morphology, and structure control. Despite the considerable advancement in this area, more studies are still required on various aspects to further promote the use of visible light magnetic heterostructure photocatalysts. The following concepts are of special importance:

(1) It is generally accepted that degradation of resistant organic air pollutants such as polycyclic aromatic hydrocarbons (PAHs), phthalate ester (PEs), and dioxins is of paramount importance for environmental air protection and indoor air purification. However, the use of visible light magnetic heterostructure photocatalysts has been studied mainly in the liquid phase rather than gaseous phase. However, visible light, especially sunlight, can be more efficiently utilized in the gaseous media. Therefore, it is necessary to expand the application of visible light magnetic heterostructure photocatalysts for the decomposition of gaseous contaminants.

(2) Previous works on magnetic-semiconductor nanocomposite heterostructure photocatalysts have mainly focused on the photocatalytic decomposition of organic pollutants (dyes, pesticides, pharmaceuticals, herbicides, and so on), while scant attention has been paid to researches on their industrialization. Using a combination of magnetic components and visible light active photocatalysts that can be synthesized by facile techniques offers a promising method to control the environmental pollution at the large scale.

References

Ai Z, Deng K, Wan Q, Zhang L, Lee S (2010) Facile microwave-assisted synthesis and magnetic and gas sensing properties of Fe_3O_4 nanoroses. J Phys Chem C 114(14):6237–6242. https://doi.org/10.1021/jp910514f

Akhundi A, Habibi-Yangjeh A (2015) Novel magnetic gC_3N_4/Fe_3O_4/AgCl nanocomposites: facile and large-scale preparation and highly efficient photocatalytic activities under visible-light irradiation. Mater Sci Semicond Process 39:162–171. https://doi.org/10.1016/j.mssp.2015.04.052

Aljubourya D, Palaniandy P, Aziz H, Feroz S (2016) Comparative study to the solar photo-Fenton, solar photocatalyst of TiO_2 and solar photocatalyst of TiO_2 combined with Fenton process to treat petroleum wastewater by RSM. J Pet Environ Biotechnol 7:2

Amara D, Grinblat J, Margel S (2012) Solventless thermal decomposition of ferrocene as a new approach for one-step synthesis of magnetite nanocubes and nanospheres. J Mater Chem 22(5):2188–2195. https://doi.org/10.1039/C1JM13942H

An C, Ming X, Wang J, Wang S (2012) Construction of magnetic visible-light-driven plasmonic $Fe_3O_4@SiO_2@AgCl$:Ag nanophotocatalyst. J Mater Chem 22(11):5171–5176. https://doi.org/10.1039/c2jm16622d

Augugliaro V, Litter M, Palmisano L, Soria J (2006) The combination of heterogeneous photocatalysis with chemical and physical operations: a tool for improving the photoprocess performance. J Photochem Photobiol C: Photochem Rev 7(4):127–144. https://doi.org/10.1016/j.jphotochemrev.2006.12.001

Bastami TR, Ahmadpour A (2016) Preparation of magnetic photocatalyst nanohybrid decorated by polyoxometalate for the degradation of a pharmaceutical pollutant under solar light. Environ Sci Pollut Res 23(9):8849–8860. https://doi.org/10.1007/s11356-015-5985-2

Bastami TR, Entezari MH (2013) High stable suspension of magnetite nanoparticles in ethanol by using sono-synthesized nanomagnetite in polyol medium. Mater Res Bull 48(9):3149–3156. https://doi.org/10.1016/j.materresbull.2013.04.067

Bayal N, Jeevanandam P (2013) Synthesis of $SiO_2@NiO$ magnetic core–shell nanoparticles and their use as adsorbents for the removal of methylene blue. J Nanopart Res 15:1–15

Bhukal S, Bansal S, Singhal S (2014) Magnetic Mn substituted cobalt zinc ferrite systems: structural, electrical and magnetic properties and their role in photo-catalytic degradation of methyl orange azo dye. Phys B Condens Matter 445:48–55. https://doi.org/10.1016/j.physb.2014.03.088

Boumaza S, Boudjemaa A, Bouguelia A, Bouarab R, Trari M (2010) Visible light induced hydrogen evolution on new hetero-system $ZnFe_2O_4/SrTiO_3$. Appl Energy 87(7):2230–2236. https://doi.org/10.1016/j.apenergy.2009.12.016

Cai A, Sun Y, Du L, Wang X (2015) Hierarchical Ag_2O–ZnO–Fe_3O_4 composites with enhanced visible-light photocatalytic activity. J Alloys Compd 644:334–340. https://doi.org/10.1016/j.jallcom.2015.03.236

Cao S, Zhou P, Yu J (2014a) Recent advances in visible light bi-based photocatalysts. Chin J Catal 35:989–1007

Cao X, Chen Y, Jiao S, Fang Z, Xu M, Liu X, Li L, Pang G, Feng S (2014b) Magnetic photocatalysts with a p–n junction: Fe_3O_4 nanoparticle and $FeWO_4$ nanowire heterostructures. Nano 6:12366–12370

Cao C, Xiao L, Chen C, Cao Q (2015a) Magnetically separable Cu_2O/chitosan–Fe_3O_4 nanocomposites: preparation, characterization and visible-light photocatalytic performance. Appl Surf Sci 333:110–118. https://doi.org/10.1016/j.apsusc.2015.02.002

Cao Y, Li C, Li J, Li Q, Yang J (2015b) Magnetically separable Fe_3O_4/AgBr hybrid materials: highly efficient photocatalytic activity and good stability. Nanoscale Res Lett 10:1

Cao Y, Li C, Li J, Li Q, Yang J (2015c) Magnetically separable Fe_3O_4/AgBr hybrid materials: highly efficient photocatalytic activity and good stability. Nanoscale Res Lett 10(1):251. https://doi.org/10.1186/s11671-015-0952-x

Casbeer E, Sharma VK, Li X-Z (2012) Synthesis and photocatalytic activity of ferrites under visible light: a review. Sep Purif Technol 87:1–14. https://doi.org/10.1016/j.seppur.2011.11.034

Chatterjee D, Dasgupta S (2005) Visible light induced photocatalytic degradation of organic pollutants. J Photochem Photobiol C: Photochem Rev 6(2-3):186–205. https://doi.org/10.1016/j.jphotochemrev.2005.09.001

Chen X, Mao SS (2007) Titanium dioxide nanomaterials: synthesis, properties, modifications, and applications. Chem Rev 107(7):2891–2959. https://doi.org/10.1021/cr0500535

Chen WJ, Tsai PJ, Chen YC (2008) Functional Fe_3O_4/TiO_2 core/shell magnetic nanoparticles as photokilling agents for pathogenic bacteria. Small 4(4):485–491. https://doi.org/10.1002/smll.200701164

Chen G, Desinan S, Nechache R, Rosei R, Rosei F, Ma D (2011) Bifunctional catalytic/magnetic Ni@Ru core–shell nanoparticles. Chem Commun 47(22):6308–6310. https://doi.org/10.1039/c1cc10619h

Chen X, Dai Y, Liu T, Guo J, Wang X, Li F (2015) Magnetic core–shell carbon microspheres (CMSs)@$ZnFe_2O_4/Ag_3PO_4$ composite with enhanced photocatalytic activity and stability under visible light irradiation. J Mol Catal A Chem 409:198–206. https://doi.org/10.1016/j.molcata.2015.08.021

Chong MN, Jin B, Chow CW, Saint C (2010) Recent developments in photocatalytic water treatment technology: a review. Water Res 44(10):2997–3027. https://doi.org/10.1016/j.watres.2010.02.039

Deng Y, Zhao R (2015) Advanced oxidation processes (AOPs) in wastewater treatment. Curr Pollut Rep 1(3):167–176. https://doi.org/10.1007/s40726-015-0015-z

Dom R, Subasri R, Radha K, Borse PH (2011) Synthesis of solar active nanocrystalline ferrite, MFe_2O_4 (M: Ca, Zn, Mg) photocatalyst by microwave irradiation. Solid State Commun 151(6):470–473. https://doi.org/10.1016/j.ssc.2010.12.034

Dong W, Zhu C (2002) Use of ethylene oxide in the sol–gel synthesis of α-Fe_2O_3 nanoparticles from Fe (III) salts. J Mater Chem 12(6):1676–1683. https://doi.org/10.1039/b200773h

Dong S, Cui Y, Wang Y, Li Y, Hu L, Sun J, Sun J (2014) Designing three-dimensional acicular sheaf shaped $BiVO_4$/reduced graphene oxide composites for efficient sunlight-driven photocatalytic degradation of dye wastewater. Chem Eng J 249:102–110. https://doi.org/10.1016/j.cej.2014.03.071

Franquet-Griell H, Medina A, Sans C, Lacorte S (2017) Biological and photochemical degradation of cytostatic drugs under laboratory conditions. J Hazard Mater 323(Pt A):319–328. https://doi.org/10.1016/j.jhazmat.2016.06.057

Fujishima A, Zhang X, Tryk DA (2007) Heterogeneous photocatalysis: from water photolysis to applications in environmental cleanup. Int J Hydrog Energy 32(14):2664–2672. https://doi.org/10.1016/j.ijhydene.2006.09.009

Gibson MA, Hightower JW (1976) Oxidative dehydrogenation of butenes over magnesium ferrite: catalyst deactivation studies. J Catal 41(3):431–439. https://doi.org/10.1016/0021-9517(76)90244-X

Goswami D (1997) A review of engineering developments of aqueous phase solar photocatalytic detoxification and disinfection processes. Trans-Am Soc Mech Eng. J Solar Energy Eng 119(2):101–107. https://doi.org/10.1115/1.2887886

Goswami DY, Trivedi DM, Block SS (1997) Photocatalytic disinfection of indoor air. J Sol Energy Eng 119(1):92–96

Guin D, Baruwati B, Manorama SV (2005) A simple chemical synthesis of nanocrystalline AFe_2O_4 (A = Fe, Ni, Zn): an efficient catalyst for selective oxidation of styrene. J Mol Catal A Chem 242(1-2):26–31. https://doi.org/10.1016/j.molcata.2005.07.021

Gutierrez-Mata A, Velazquez-Martínez S, Álvarez-Gallegos A, Ahmadi M, Hernández-Pérez JA, Ghanbari F, Silva-Martínez S (2017) Recent overview of solar photocatalysis and solar photo-Fenton processes for wastewater treatment. Int J Photoenergy 2017:1–27. https://doi.org/10.1155/2017/8528063

Hamad H, El-Latif MA, Kashyout AE-H, Sadik W, Feteha M (2015) Synthesis and characterization of core–shell–shell magnetic ($CoFe_2O_4$–SiO_2–TiO_2) nanocomposites and TiO_2 nanoparticles for the evaluation of photocatalytic activity under UV and visible irradiation. New J Chem 39(4):3116–3128. https://doi.org/10.1039/C4NJ01821D

Han L-H, Liu H, Wei Y (2011) In situ synthesis of hematite nanoparticles using a low-temperature microemulsion method. Powder Technol 207(1-3):42–46. https://doi.org/10.1016/j.powtec.2010.10.008

Hankare P, Patil R, Jadhav A, Garadkar K, Sasikala R (2011) Enhanced photocatalytic degradation of methyl red and thymol blue using titania–alumina–zinc ferrite nanocomposite. Appl Catal B Environ 107(3-4):333–339. https://doi.org/10.1016/j.apcatb.2011.07.033

Hidalgo M, Murcia J, Navío J, Colón G (2011) Photodeposition of gold on titanium dioxide for photocatalytic phenol oxidation. Appl Catal A Gen 397(1-2):112–120. https://doi.org/10.1016/j.apcata.2011.02.030

Hoffmann MR, Martin ST, Choi W, Bahnemann DW (1995) Environmental applications of semiconductor photocatalysis. Chem Rev 95(1):69–96. https://doi.org/10.1021/cr00033a004

Huang S, Xu Y, Chen Z, Xie M, Xu H, He M, Li H, Zhang Q (2015a) A core–shell structured magnetic Ag/AgBr@Fe_2O_3 composite with enhanced photocatalytic activity for organic pollutant degradation and antibacterium. RSC Adv 5(87):71035–71045. https://doi.org/10.1039/C5RA13403J

Huang S, Xu Y, Xie M, Xu H, He M, Xia J, Huang L, Li H (2015b) Synthesis of magnetic $CoFe_2O_4/gC_3N_4$ composite and its enhancement of photocatalytic ability under visible-light. Colloids Surf A Physicochem Eng Asp 478:71–80. https://doi.org/10.1016/j.colsurfa.2015.03.035

Ibhadon AO, Fitzpatrick P (2013) Heterogeneous photocatalysis: recent advances and applications. Catalysts 3(1):189–218. https://doi.org/10.3390/catal3010189

Ida S, Yamada K, Matsunaga T, Hagiwara H, Matsumoto Y, Ishihara T (2010) Preparation of p-type $CaFe_2O_4$ photocathodes for producing hydrogen from water. J Am Chem Soc 132:17343–17345

Jang I, You K-E, Kim YC, Oh S-G (2014) Surfactant-assisted preparation of core-shell-type TiO_2–Fe_2O_3 composites and their photocatalytic activities under room light irradiation. Appl Surf Sci 316:187–193. https://doi.org/10.1016/j.apsusc.2014.07.204

Jiang J, Tang X, Zhou S, Ding J, Zhou H, Zhang F, Zhang D, Fan T (2016) Synthesis of visible and near infrared light sensitive amorphous titania for photocatalytic hydrogen evolution. Green Chem 18(7):2056–2062. https://doi.org/10.1039/C5GC02170G

Kitano M, Hara M (2010) Heterogeneous photocatalytic cleavage of water. J Mater Chem 20(4):627–641. https://doi.org/10.1039/B910180B

Kong L, Wang C, Gong F, Zhu W, Zhong Y, Ye X, Li F (2016) Magnetic core–shell nanostructured palladium catalysts for green oxidation of benzyl alcohol. Catal Lett 146(7):1321–1330

Ladj R, Bitar A, Eissa M, Mugnier Y, Le Dantec R, Fessi H, Elaissari A (2013) Individual inorganic nanoparticles: preparation, functionalization and in vitro biomedical diagnostic applications. J Mater Chem B 1(10):1381–1396. https://doi.org/10.1039/c2tb00301e

Laurent S, Forge D, Port M, Roch A, Robic C, Vander Elst L, Muller RN (2008) Magnetic iron oxide nanoparticles: synthesis, stabilization, vectorization, physicochemical characterizations, and biological applications. Chem Rev 108(6):2064–2110. https://doi.org/10.1021/cr068445e

Leng C, Wei J, Liu Z, Xiong R, Pan C, Shi J (2013a) Facile synthesis of PANI-modified $CoFe_2O_4$–TiO_2 hierarchical flower-like nanoarchitectures with high photocatalytic activity. J Nanopart Res 15:1–11

Leng C, Wei J, Liu Z, Xiong R, Pan C, Shi J (2013b) Facile synthesis of PANI-modified $CoFe_2O_4$–TiO_2 hierarchical flower-like nanoarchitectures with high photocatalytic activity. J Nanopart Res 15(5):1643. https://doi.org/10.1007/s11051-013-1643-0

Li Z, Lai X, Wang H, Mao D, Xing C, Wang D (2009) General synthesis of homogeneous hollow core−shell ferrite microspheres. J Phys Chem C 113(7):2792–2797. https://doi.org/10.1021/jp8094787

Li X, Niu C, Huang D, Wang X, Zhang X, Zeng G, Niu Q (2013) Preparation of magnetically separable Fe_3O_4/BiOI nanocomposites and its visible photocatalytic activity. Appl Surf Sci 286:40–46. https://doi.org/10.1016/j.apsusc.2013.08.139

Li Z-Q, Wang H-L, Zi L-Y, Zhang J-J, Zhang Y-S (2015) Preparation and photocatalytic performance of magnetic TiO_2–Fe_3O_4/graphene (RGO) composites under VIS-light irradiation. Ceram Int 41(9): 10634–10643. https://doi.org/10.1016/j.ceramint.2015.04.163

Link H, Turchi CS (1991) Cost and performance projections for solar water detoxification systems. Asme Jses Jsme Int Sol Energ Conf 289–294

Liu L, Li Y (2014) Understanding the reaction mechanism of photocatalytic reduction of CO_2 with H_2O on TiO_2-based photocatalysts: a review. Aerosol Air Qual Res 14:453–469

Liu S, Yu J, Jaroniec M (2011) Anatase TiO_2 with dominant high-energy {001} facets: synthesis, properties, and applications. Chem Mater 23(18):4085–4093. https://doi.org/10.1021/cm200597m

Liu Y, Yu L, Hu Y, Guo C, Zhang F, Lou XWD (2012a) A magnetically separable photocatalyst based on nest-like γ-Fe_2O_3/ZnO double-shelled hollow structures with enhanced photocatalytic activity. Nano 4:183–187

Liu Z, Xu W, Fang J, Xu X, Wu S, Zhu X, Chen Z (2012b) Decoration of BiOI quantum size nanoparticles with reduced graphene oxide in enhanced visible-light-driven photocatalytic studies. Appl Surf Sci 259:441–447. https://doi.org/10.1016/j.apsusc.2012.07.063

Liu J, Xu J, Che R, Chen H, Liu M, Liu Z (2013) Hierarchical Fe_3O_4@TiO_2 yolk–shell microspheres with enhanced microwave-absorption properties. Chem—Eur J 19(21):6746–6752. https://doi.org/10.1002/chem.201203557

Liŭ D, Li Z, Wang W, Wang G, Liú D (2016) Hematite doped magnetic TiO_2 nanocomposites with improved photocatalytic activity. J Alloys Compd 654:491–497. https://doi.org/10.1016/j.jallcom.2015.09.140

Liu Y, Yu Z, Peng Z, Xiang G, Sun L, Gong Z, Zhu J, Su D, Liu Y (2016) Degradation of methyl orange by simulated solar light combined with three-dimensional electro-Fenton system. Chin J Environ Eng 10:1727–1734

Lu C, Chung Y-L, Chang K-F (2005) Adsorption of trihalomethanes from water with carbon nanotubes. Water Res 39(6):1183–1189. https://doi.org/10.1016/j.watres.2004.12.033

Lu AH, Salabas EL, Schüth F (2007) Magnetic nanoparticles: synthesis, protection, functionalization, and application. Angew Chem Int Ed 46(8):1222–1244. https://doi.org/10.1002/anie.200602866

Magara Y, Aizawa T, Matumoto N, Souna F (1994) Degradation of pesticides by chlorination during water purification. Water Sci Technol 30:119–128

Mahmoodi V, Sargolzaei J (2014a) Photocatalytic abatement of naphthalene catalyzed by nanosized TiO_2 particles: assessment of operational parameters. Theor Found Chem Eng 48(5):656–666. https://doi.org/10.1134/S0040579514050194

Mahmoodi V, Sargolzaei J (2014b) Optimization of photocatalytic degradation of naphthalene using nano-TiO_2/UV system: statistical analysis by a response surface methodology. Desalin Water Treat 52(34-36):6664–6672. https://doi.org/10.1080/19443994.2013.861774

Mahmoodi V, Ahmadpour A, Rohani Bastami T, Hamed Mousavian MT (2017) Facile synthesis of BiOI nanoparticles at room temperature and evaluation of their photoactivity under sunlight irradiation. Photochem Photobiol. https://doi.org/10.1111/php.12832

Malato S, Fernández-Ibáñez P, Maldonado M, Blanco J, Gernjak W (2009) Decontamination and disinfection of water by solar photocatalysis: recent overview and trends. Catal Today 147(1):1–59. https://doi.org/10.1016/j.cattod.2009.06.018

Manova E, Tsoncheva T, Paneva D, Mitov I, Tenchev K, Petrov L (2004) Mechanochemically synthesized nano-dimensional iron–cobalt spinel oxides as catalysts for methanol decomposition. Appl Catal A Gen 277(1-2):119–127. https://doi.org/10.1016/j.apcata.2004.09.002

Marcucci M, Nosenzo G, Capannelli G, Ciabatti I, Corrieri D, Ciardelli G (2001) Treatment and reuse of textile effluents based on new ultrafiltration and other membrane technologies. Desalination 138(1-3): 75–82. https://doi.org/10.1016/S0011-9164(01)00247-8

Markides H, Rotherham M, El Haj A (2012) Biocompatibility and toxicity of magnetic nanoparticles in regenerative medicine. J Nanomater 2012:13

Martyanov IN, Uma S, Rodrigues S, Klabunde KJ (2004) Structural defects cause TiO_2-based photocatalysts to be active in visible light. Chem Commun 10(21):2476–2477. https://doi.org/10.1039/b409730k

Mascolo MC, Pei Y, Ring TA (2013) Room temperature co-precipitation synthesis of magnetite nanoparticles in a large pH window with different bases. Materials 6(12):5549–5567. https://doi.org/10.3390/ma6125549

Massart R (1981) Preparation of aqueous magnetic liquids in alkaline and acidic media. IEEE Trans Magn 17(2):1247–1248. https://doi.org/10.1109/TMAG.1981.1061188

Mou F, Xu L, Ma H, Guan J, Chen D-r, Wang S (2012) Facile preparation of magnetic γ-Fe_2O_3/TiO_2 Janus hollow bowls with efficient visible-light photocatalytic activities by asymmetric shrinkage. Nano 4:4650–4657

Nakada N, Tanishima T, Shinohara H, Kiri K, Takada H (2006) Pharmaceutical chemicals and endocrine disrupters in municipal wastewater in Tokyo and their removal during activated sludge treatment. Water Res 40(17):3297–3303. https://doi.org/10.1016/j.watres.2006.06.039

Naseroleslami M, Parivar K, Khoei S, Aboutaleb N (2016) Magnetic resonance imaging of human-derived amniotic membrane stem cells using PEGylated superparamagnetic iron oxide nanoparticles. Cell J (Yakhteh) 18:332

Ndounla J, Pulgarin C (2015) Solar light (hν) and H_2O_2/hν photodisinfection of natural alkaline water (pH 8.6) in a compound parabolic collector at different day periods in Sahelian region. Environ Sci Pollut Res 22(21):17082–17094. https://doi.org/10.1007/s11356-015-4784-0

Ni M, Leung MK, Leung DY, Sumathy K (2007) A review and recent developments in photocatalytic water-splitting using TiO_2 for hydrogen production. Renew Sust Energ Rev 11(3):401–425. https://doi.org/10.1016/j.rser.2005.01.009

Oller I, Gernjak W, Maldonado M, Pérez-Estrada L, Sánchez-Pérez J, Malato S (2006) Solar photocatalytic degradation of some hazardous water-soluble pesticides at pilot-plant scale. J Hazard Mater 138(3):507–517. https://doi.org/10.1016/j.jhazmat.2006.05.075

Oppenländer T (2003) Photochemical purification of water and air: advanced oxidation processes (AOPs)-principles, reaction mechanisms, Reactor Concepts. John Wiley & Sons, Hoboken

Park J, Lee E, Hwang NM, Kang M, Kim SC, Hwang Y, Park JG, Noh HJ, Kim JY, Park JH (2005) One-nanometer-scale size-controlled synthesis of monodisperse magnetic iron oxide nanoparticles. Angew Chem 117(19):2932–2937. https://doi.org/10.1002/ange.200461665

Qi H, Yan B, Lu W, Li C, Yang Y (2011) A non-alkoxide sol-gel method for the preparation of magnetite (Fe_3O_4) nanoparticles. Curr Nanosci 7(3):381–388. https://doi.org/10.2174/157341311795542426

Qu Y, Duan X (2013) Progress, challenge and perspective of heterogeneous photocatalysts. Chem Soc Rev 42(7):2568–2580. https://doi.org/10.1039/C2CS35355E

Rajeshwar K, Osugi M, Chanmanee W, Chenthamarakshan C, Zanoni MVB, Kajitvichyanukul P, Krishnan-Ayer R (2008) Heterogeneous photocatalytic treatment of organic dyes in air and aqueous media. J Photochem Photobiol C: Photochem Rev 9(4):171–192. https://doi.org/10.1016/j.jphotochemrev.2008.09.001

Ratner BD, Hoffman AS, Schoen FJ, Lemons JE (2006) Biomaterials science: an introduction to materials in medicine. MRS Bull 31:59

Reddy LH, Arias JL, Nicolas J, Couvreur P (2012) Magnetic nanoparticles: design and characterization, toxicity and biocompatibility, pharmaceutical and biomedical applications. Chem Rev 112(11): 5818–5878. https://doi.org/10.1021/cr300068p

Rosenfeldt EJ, Linden KG (2004) Degradation of endocrine disrupting chemicals bisphenol A, ethinyl estradiol, and estradiol during UV photolysis and advanced oxidation processes. Environ Sci Technol 38(20):5476–5483. https://doi.org/10.1021/es035413p

Rui Z, Jingguo W, Jianyu C, Lin H, Kangguo M (2010) Photocatalytic degradation of pesticide residues with RE^{3+}-doped nano-TiO_2. J Rare Earths 28:353–356

Salgado SYA, Zamora RMR, Zanella R, Peral J, Malato S, Maldonado MI (2016) Photocatalytic hydrogen production in a solar pilot plant using a Au/TiO_2 photo catalyst. Int J Hydrog Energy 41(28):11933–11940. https://doi.org/10.1016/j.ijhydene.2016.05.039

Sathishkumar P, Mangalaraja RV, Anandan S, Ashokkumar M (2013) $CoFe_2O_4$/TiO_2 nanocatalysts for the photocatalytic degradation of Reactive Red 120 in aqueous solutions in the presence and absence of electron acceptors. Chem Eng J 220:302–310. https://doi.org/10.1016/j.cej.2013.01.036

Scheffel A, Gruska M, Faivre D, Linaroudis A, Plitzko JM, Schüler D (2006) An acidic protein aligns magnetosomes along a filamentous structure in magnetotactic bacteria. Nature 440(7080):110–114. https://doi.org/10.1038/nature04382

Shaban YA, El Sayed MA, El Maradny AA, Al Farawati RK, Al Zobidi MI, Khan SU (2016) Laboratory and pilot-plant scale photocatalytic degradation of polychlorinated biphenyls in seawater using CM-n-TiO_2 nanoparticles. Int J Photoenergy 2016:1–7. https://doi.org/10.1155/2016/8471960

Shekofteh-Gohari M, Habibi-Yangjeh A (2015) Novel magnetically separable Fe_3O_4@ZnO/AgCl nanocomposites with highly enhanced photocatalytic activities under visible-light irradiation. Sep Purif Technol 147:194–202. https://doi.org/10.1016/j.seppur.2015.04.034

Shi Z, Xiang Y, Zhang X, Yao S (2011) Photocatalytic activity of Ho-doped anatase titanium dioxide coated magnetite. Photochem Photobiol 87(3):626–631. https://doi.org/10.1111/j.1751-1097.2011.00893.x

Shiraishi K, Koseki H, Tsurumoto T, Baba K, Naito M, Nakayama K, Shindo H (2009) Antibacterial metal implant with a TiO_2-conferred photocatalytic bactericidal effect against *Staphylococcus aureus*. Surf Interface Anal 41(1):17–22. https://doi.org/10.1002/sia.2965

Shojaei AF, Shams-Nateri A, Ghomashpasand M (2015) Comparative study of photocatalytic activities of magnetically separable WO_3/TiO_2/Fe_3O_4 nanocomposites and TiO_2, WO_3/TiO_2 and TiO_2/Fe_3O_4 under visible light irradiation. Superlattice Microst 88:211–224. https://doi.org/10.1016/j.spmi.2015.09.014

Singh S, Barick K, Bahadur D (2013) Fe_3O_4 embedded ZnO nanocomposites for the removal of toxic metal ions, organic dyes and bacterial pathogens. J Mater Chem A 1(10):3325–3333. https://doi.org/10.1039/c2ta01045c

Spasiano D, Rodriguez LPP, Olleros JC, Malato S, Marotta R, Andreozzi R (2013) TiO_2/Cu (II) photocatalytic production of benzaldehyde from benzyl alcohol in solar pilot plant reactor. Appl Catal B Environ 136:56–63

Stasinakis A (2008) Use of selected advanced oxidation processes (AOPs) for wastewater treatment—a mini review. Global NEST J 10:376–385

Suh SK, Yuet K, Hwang DK, Bong KW, Doyle PS, Hatton TA (2012) Synthesis of nonspherical superparamagnetic particles: in situ coprecipitation of magnetic nanoparticles in microgels prepared by stop-flow lithography. J Am Chem Soc 134(17):7337–7343. https://doi.org/10.1021/ja209245v

Sun A, Xiong Z, Xu Y (2008) Removal of malodorous organic sulfides with molecular oxygen and visible light over metal phthalocyanine. J Hazard Mater 152(1):191–195. https://doi.org/10.1016/j.jhazmat.2007.06.105

Tang J, Zou Z, Ye J (2004) Efficient photocatalytic decomposition of organic contaminants over $CaBi_2O_4$ under visible-light irradiation. Angew Chem Int Ed 43(34):4463–4466. https://doi.org/10.1002/anie.200353594

Tang H, Zhang D, Tang G, Ji X, Li W, Li C, Yang X (2013) Hydrothermal synthesis and visible-light photocatalytic activity of α-Fe_2O_3/TiO_2 composite hollow microspheres. Ceram Int 39(8):8633–8640. https://doi.org/10.1016/j.ceramint.2013.04.040

Tang W, Su Y, Wang X, Li Q, Gao S, Shang JK (2014) Synthesis of a superparamagnetic MFNs@SiO_2@$Ag_4SiW_{12}O_{40}$/Ag composite photocatalyst, its superior photocatalytic performance under visible light illumination, and its easy magnetic separation. RSC Adv 4(57): 30090–30099. https://doi.org/10.1039/C4RA03711A

Tanhaei B, Ayati A, Lahtinen M, Mahmoodzadeh Vaziri B, Sillanpää M (2016) A magnetic mesoporous chitosan based core-shells biopolymer for anionic dye adsorption: kinetic and isothermal study and application of ANN. J Appl Polym Sci 133(22):1–11

Theurich J, Bahnemann D, Vogel R, Ehamed F, Alhakimi G, Rajab I (1997) Photocatalytic degradation of naphthalene and anthracene: GC-MS analysis of the degradation pathway. Res Chem Intermed 23(3):247–274. https://doi.org/10.1163/156856797X00457

Tian Y, Yu B, Li X, Li K (2011) Facile solvothermal synthesis of monodisperse Fe_3O_4 nanocrystals with precise size control of one nanometre as potential MRI contrast agents. J Mater Chem 21(8): 2476–2481. https://doi.org/10.1039/c0jm02913k

Toepfer B, Gora A, Puma GL (2006) Photocatalytic oxidation of multicomponent solutions of herbicides: reaction kinetics analysis with explicit photon absorption effects. Appl Catal B Environ 68(3-4): 171–180. https://doi.org/10.1016/j.apcatb.2006.06.020

Topac BS, Alkan U (2016) Comparison of solar/H_2O_2 and solar photo-fenton processes for the disinfection of domestic wastewaters. KSCE J Civ Eng 20(7):2632–2639. https://doi.org/10.1007/s12205-016-0416-6

Trapido M, Hirvonen A, Veressinina Y, Hentunen J, Munter R (1997) Ozonation, ozone/UV and UV/H O degradation of chlorophenols. Ozone Sci Eng 19(1):75–96

Vanga PR, Mangalaraja R, Ashok M (2015) Structural, magnetic and photocatalytic properties of La and alkaline co-doped $BiFeO_3$ nanoparticles. Mater Sci Semicond Process 40:796–802. https://doi.org/10.1016/j.mssp.2015.07.078

Villa K, Domènech X, Malato S, Maldonado MI, Peral J (2013) Heterogeneous photocatalytic hydrogen generation in a solar pilot plant. Int J Hydrog Energy 38(29):12718–12724. https://doi.org/10.1016/j.ijhydene.2013.07.046

Wang C, Xu C, Zeng H, Sun S (2009a) Recent progress in syntheses and applications of dumbbell-like nanoparticles. Adv Mater 21(30): 3045–3052. https://doi.org/10.1002/adma.200900320

Wang C, Yin L, Zhang L, Kang L, Wang X, Gao R (2009b) Magnetic (γ-Fe_2O_3@ SiO_2)n@TiO_2 functional hybrid nanoparticles with actived photocatalytic ability. J Phys Chem C 113(10):4008–4011. https://doi.org/10.1021/jp809835a

Wang H, Hu Y, Jiang Y, Qiu L, Wu H, Guo B, Shen Y, Wang Y, Zhu L, Xie A (2013) Facile synthesis and excellent recyclable photocatalytic activity of pine cone-like Fe_3O_4@Cu_2O/Cu porous nanocomposites. Dalton Trans 42(14):4915–4921. https://doi.org/10.1039/c2dt32290k

Wang X, Li X, Li X, Xu L, Liu Z, Duan L, Liu J (2014) Electrospun TiO_2 nanofibers integrating space-separated magnetic nanoparticles and heterostructures for recoverable and efficient photocatalyst. J Mater Chem A 2:12304–12310

Wang M, Wei N, Fu W, Yan M, Long L, Yao Y, Yin G, Liao X, Huang Z, Chen X (2015) An efficient and recyclable urchin-like yolk–shell Fe_3O_4@SiO_2@Co_3O_4 catalyst for photocatalytic water oxidation. Catal Lett 145(4):1067–1071. https://doi.org/10.1007/s10562-015-1501-z

Wu W, Xiao X, Zhang S, Zhou J, Fan L, Ren F, Jiang C (2010) Large-scale and controlled synthesis of iron oxide magnetic short nanotubes: shape evolution, growth mechanism, and magnetic properties. J Phys Chem C 114(39):16092–16103. https://doi.org/10.1021/jp1010154

Wu L, Yao H, Hu B, Yu S-H (2011) Unique lamellar sodium/potassium iron oxide nanosheets: facile microwave-assisted synthesis and magnetic and electrochemical properties. Chem Mater 23(17):3946–3952. https://doi.org/10.1021/cm2013736

Wu W, Liao L, Zhang S, Zhou J, Xiao X, Ren F, Sun L, Dai Z, Jiang C (2013) Non-centrosymmetric Au–SnO_2 hybrid nanostructures with strong localization of plasmonic for enhanced photocatalysis application. Nano 5:5628–5636

Wu W, Jiang C, Roy VA (2015) Recent progress in magnetic iron oxide–semiconductor composite nanomaterials as promising photocatalysts. Nano 7:38–58

Xi G, Yue B, Cao J, Ye J (2011) Fe_3O_4/WO_3 hierarchical core–shell structure: high-performance and recyclable visible-light photocatalysis. Chem—Eur J 17(18):5145–5154. https://doi.org/10.1002/chem.201002229

Xu S, Shangguan W, Yuan J, Shi J, Chen M (2007) Preparations and photocatalytic degradation of methyl orange in water on magnetically separable $Bi_{12}TiO_{20}$ supported on nickel ferrite. Sci Technol Adv Mater 8(1-2):40–46. https://doi.org/10.1016/j.stam.2006.09.009

Xu S, Feng D, Shangguan W (2009) Preparations and photocatalytic properties of visible-light-active zinc ferrite-doped TiO_2 photocatalyst. J Phys Chem C 113(6):2463–2467. https://doi.org/10.1021/jp806704y

Xu P, Zeng GM, Huang DL, Feng CL, Hu S, Zhao MH, Lai C, Wei Z, Huang C, Xie GX (2012) Use of iron oxide nanomaterials in wastewater treatment: a review. Sci Total Environ 424:1–10. https://doi.org/10.1016/j.scitotenv.2012.02.023

Yan Y, Sun S, Song Y, Yan X, Guan W, Liu X, Shi W (2013) Microwave-assisted in situ synthesis of reduced graphene oxide-$BiVO_4$ composite photocatalysts and their enhanced photocatalytic performance for the degradation of ciprofloxacin. J Hazard Mater 250:106–114

Yang J, Chen C, Ji H, Ma W, Zhao J (2005) Mechanism of TiO_2-assisted photocatalytic degradation of dyes under visible irradiation: photoelectrocatalytic study by TiO_2-film electrodes. J Phys Chem B 109(46):21900–21907. https://doi.org/10.1021/jp0540914

Yao YR, Huang WZ, Zhou H, Cui X, Zheng YF, Song XC (2014a) Synthesis of core–shell nanostructured magnetic photocatalyst Fe_3O_4@SiO_2@Ag_3PO_4 with excellent visible-light-responding photocatalytic activity. J Nanopart Res 16:1–10

Yao YR, Huang WZ, Zhou H, Cui X, Zheng YF, Song XC (2014b) Synthesis of core–shell nanostructured magnetic photocatalyst Fe_3O_4@SiO_2@Ag_3PO_4 with excellent visible-light-responding photocatalytic activity. J Nanopart Res 16(11):2742. https://doi.org/10.1007/s11051-014-2742-2

Yeber M, Rodríguez J, Freer J, Baeza J, Durán N, Mansilla HD (1999) Advanced oxidation of a pulp mill bleaching wastewater. Chemosphere 39(10):1679–1688. https://doi.org/10.1016/S0045-6535(99)00068-5

Yoon S, Krishnan KM (2011) Temperature dependence of magnetic anisotropy constant in manganese ferrite nanoparticles at low temperature. J Appl Phys 109:07B534

Yu JC, Ho W, Lin J, Yip H, Wong PK (2003) Photocatalytic activity, antibacterial effect, and photoinduced hydrophilicity of TiO_2 films coated on a stainless steel substrate. Environ Sci Technol 37:2296–2301

Yu L, Yang X, Wang D (2015) TiO_2 incorporated in magnetic mesoporous SBA-15 by a facile inner-pore hydrolysis process toward enhanced adsorption–photocatalysis performances for As (III). J Colloid Interface Sci 448:525–532. https://doi.org/10.1016/j.jcis.2015.02.071

Zapata-Torres M, Hernández-Rodríguez E, Mis-Fernandez R, Meléndez-Lira M, Amaya OC, Bahena D, Rejon V, Peña J (2015) Visible and infrared photocatalytic activity of TiO_x thin films prepared by reactive sputtering. Mater Sci Semicond Process 40:720–726. https://doi.org/10.1016/j.mssp.2015.07.072

Zeng L, Ren W, Xiang L, Zheng J, Chen B, Wu A (2013) Multifunctional Fe_3O_4–TiO_2 nanocomposites for magnetic resonance imaging and potential photodynamic therapy. Nano 5:2107–2113

Zhang T, Yan X, Sun DD (2012) Hierarchically multifunctional K-OMS-2/TiO_2/Fe_3O_4 heterojunctions for the photocatalytic oxidation of humic acid under solar light irradiation. J Hazard Mater 243:302–310. https://doi.org/10.1016/j.jhazmat.2012.10.037

Zhang C, Wang H, Liu F, Wang L, He H (2013) Magnetic core–shell Fe_3O_4@C-SO_3H nanoparticle catalyst for hydrolysis of cellulose. Cellulose 20(1):127–134. https://doi.org/10.1007/s10570-012-9839-5

Zhang Y, Lin X, Zhou Q, Luo X (2016) Fluoride adsorption from aqueous solution by magnetic core-shell Fe_3O_4@ alginate-La particles fabricated via electro-coextrusion. Appl Surf Sci 389:34–45. https://doi.org/10.1016/j.apsusc.2016.07.087

Zhongliang S, Xingman Y, Shuhua Y (2012) Photocatalytic activity of cerium-doped mesoporous TiO_2 coated Fe_3O_4 magnetic composite under UV and visible light. J Rare Earths 30:355–360

Zhou Y, Zhu Y, Yang X, Huang J, Chen W, Lv X, Li C, Li C (2015) Au decorated Fe_3O_4@TiO_2 magnetic composites with visible light-assisted enhanced catalytic reduction of 4-nitrophenol. RSC Adv 5(62):50454–50461. https://doi.org/10.1039/C5RA08243A

Zhu S, Xu T, Fu H, Zhao J, Zhu Y (2007) Synergetic effect of Bi_2WO_6 photocatalyst with C_{60} and enhanced photoactivity under visible irradiation. Environ Sci Technol 41(17):6234–6239. https://doi.org/10.1021/es070953y